ORNL-5080

Twin Boundary Cavitation in Aged Type 304 Stainless Steel

V. K. Sikka
R. W. Swindeman
C. R. Brinkman

OAK RIDGE NATIONAL LABORATORY

BLANK PAGE

Printed in the United States of America. Available from
National Technical Information Service
U.S. Department of Commerce
5285 Port Royal Road, Springfield, Virginia 22161
Price: Printed Copy $4.00; Microfiche $2.25

TRANSITION FROM INTERCRYSTALLINE TO TWIN BOUNDARY CAVITATION IN T

GRAIN BOUNDARY CAVITATION

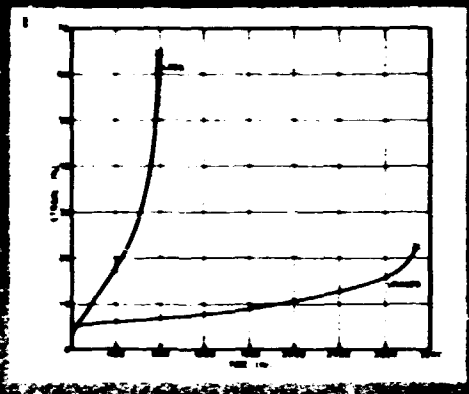

Classical creep rupture is associated with intercrystalline cracks and low ductility. Long term thermal aging (10,000 hr at 649°C) of type 304 stainless has resulted in transition from intercrystalline to annealing twin boundary cracking with a large increase in ductility. The transition from intercrystalline to twin boundary cracking is illustrated.

Fig. No.

1 Creep curves at [illegible] MPa and 593°C for both unaged and aged condition. Note loss in rupture life by a factor of four and increase in elongation by a factor of three.

2,3 Fractured specimens. Compare the location and extend of cavitation.

4,5,6,7, 8,9 Showing typical grain boundary and twin cracks. Note the nature of twin crack mark by "a" in 7 and crack "b" in 7 and 9, showing the twin crack propagation from one grain to another.

10,11 Showing the shape and size of precipitates at the grain boundaries (where cracking occurs) in the unaged specimen to be similar to shape and size of precipitates at the twin boundaries, where cracking occurs in the aged specimen.

12 Showing classical grain boundary sliding mechanism for intercrystalline cracking in the unaged specimen.

13 Showing a possible incoherent twin boundary sliding mechanism to produce cracking along the coherent part of the twin (compare with "a" in 7). Some twin cracking occurs without the presence of incoherent part of the twin and is thought to have resulted from gross intragranular deformation.

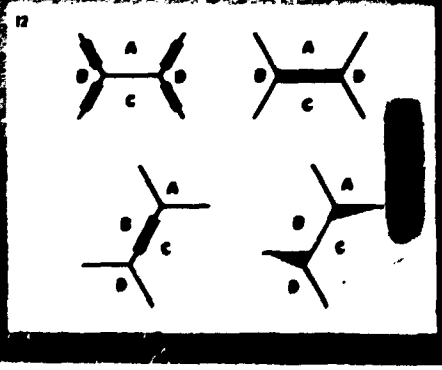

THIS DISPLAY WON FOR V. K. SIKKA AND E. H. LEE FIRST PLACE IN THE OPTICAL MICROSCOPY CLASS AT THE INTERNATIONAL METALLOGRAPHIC CONVENTION, JOINTLY SPONSORED BY THE INTERNATIONAL METALLOGRAPHIC SOCIETY AND THE AMERICAN SOCIETY FOR METALS AND HELD IN MINNEAPOLIS, MINNESOTA, JUNE 29–JULY 2, 1975.

TO TWIN BOUNDARY CAVITATION IN TYPE 304 STAINLESS STEEL

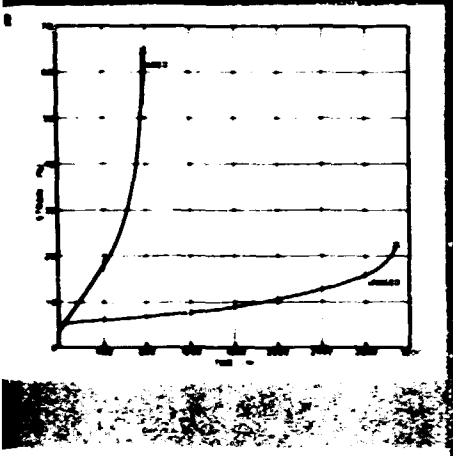

Classical creep rupture is associated with intercrystalline cracks and low ductility. Long term thermal aging (10,000 hr at 649°C) of type 304 stainless has resulted in transition from intercrystalline to annealing twin boundary cracking with a large increase in ductility. The transition from intercrystalline to twin boundary cracking is illustrated.

Fig. No.

1 Creep curves at 207 MPa and 593°C for both unaged and aged condition. Note loss in rupture life by a factor of four and increase in elongation by a factor of three.

2,3 Fractured specimens. Compare the location and extend of cavitation.

4,5,6,7, 8,9 Showing typical grain boundary and twin cracks. Note the nature of twin crack mark by "a" in 7 and crack "b" in 7 and 8, showing the twin crack propagation from one grain to another.

10,11 Showing the shape and size of precipitates at the grain boundaries (where cracking occurs) in the unaged specimen to be similar to shape and size of precipitates at the twin boundaries, where cracking occurs in the aged specimen.

12 Showing classical grain boundary sliding mechanism for intercrystalline cracking in the unaged specimen.

13 Showing a possible incoherent twin boundary sliding mechanism to produce cracking along the coherent part of the twin (compare with "a" in 7). Some twin cracking occurs without the presence of incoherent part of the twin and is thought to have resulted from gross intragranular deformation.

TWIN BOUNDARY CAVITATION

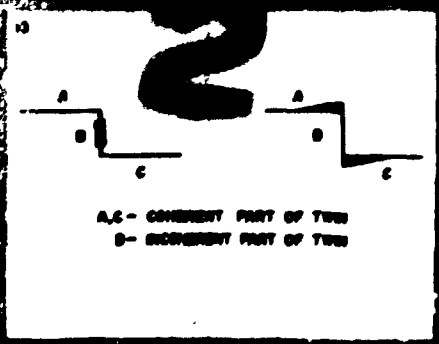

PLAY WON FOR V. K. SIKKA AND E. H. LEE
E IN THE OPTICAL MICROSCOPY CLASS AT THE
ONAL METALLOGRAPHIC CONVENTION, JOINTLY
Y THE INTERNATIONAL METALLOGRAPHIC SOCIETY
MERICAN SOCIETY FOR METALS AND HELD IN
LIS, MINNESOTA, JUNE 29–JULY 2, 1975.

ORNL-5080
UC-79b, -k
(Liquid Metal Fast
Breeder Reactors)

Contract No. W-7405-eng-26

METALS AND CERAMICS DIVISION

TWIN BOUNDARY CAVITATION IN AGED TYPE 304 STAINLESS STEEL

V. K. Sikka, R. W. Swindeman, and C. R. Brinkman

OCTOBER 1975

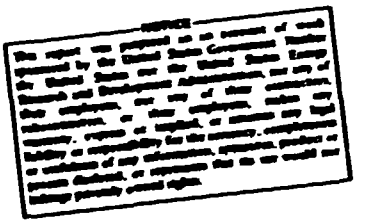

OAK RIDGE NATIONAL LABORATORY
Oak Ridge, Tennessee 37830
operated by
UNION CARBIDE CORPORATION
for the
U.S. ENERGY RESEARCH AND DEVELOPMENT ADMINISTRATION

CONTENTS

TWIN BOUNDARY CAVITATION IN AGED TYPE 304 STAINLESS STEEL

V. K. Sikka, R. W. Swindeman, and C. R. Brinkman

ABSTRACT

A transition from grain to twin boundary cavitation was observed in aged-and-creep-tested type 304 stainless steel. Evidence of twin boundary cavitation has also been observed for unaged material under certain test conditions. This same behavior was also found in aged type 316 stainless steel. Several possible reasons have been suggested for the absence of frequently observed grain boundary cavitation.

INTRODUCTION

Excellent reviews[1–5] are available in the literature on creep failure modes of metals and alloys. The most common feature of the available literature on this subject is that it refers to two basic failure modes: transgranular and intergranular. The transgranular mode is suggested to occur at low temperatures and high strain rates, whereas intergranular fracture occurs at high temperatures and low strain rates. During creep at elevated temperature, intergranular fracture is commonly observed and is suggested to occur by grain boundary sliding. The transition from transgranular to intergranular fracture is associated with a noticeable loss of ductility. Intergranular fracture involves the nucleation and growth of grain boundary cracks and voids. Garofalo[3] in his review paper listed the following grain boundary locations for nucleation of cracks and voids:

---

[1]D. A. Woodford and R. M. Goldhoff, "An Approach to the Understanding of Brittle Behavior of Steel at Elevated Temperatures," *Mater. Sci. Eng.* 5: 303–24 (1969–70).

[2]F. Garofalo, *Fundamentals of Creep and Creep-Rupture in Metals*, Macmillan, New York, 1965.

[3]F. Garofalo, *Ductility*, American Society for Metals, Metals Park, Ohio, 1968, pp. 87–129.

[4]C. Zener, *Elasticity and Inelasticity of Metals*, University of Chicago Press, Chicago, 1948.

[5]D. McLean, "The Physics of High Temperature Creep in Metals," *Rep. Progr. Phys.* 29 (Part I): 1–33 (1966).

1. triple points of high-angle boundaries,
2. inclusions and precipitate particles,
3. grain boundary ledges, and
4. junction between subboundaries and grain boundaries.

Kemsley[6] investigated the crack paths in fatigued copper and found that cracks nucleated not only along grain boundaries but also along striations and annealing twins. In a recent paper, Michel et al.[7] have shown deformation-induced crack formation at twin boundaries in type 304 stainless steel. They suggested that since cracks form along them the twin boundaries may behave in a manner similar to grain boundaries under proper conditions. The observations of Michel et al. were restricted to type 304 stainless steel tested at 650°C (1200°F) in tensile and creep tests at deformation rates between 8.33×10^{-4} and 4.6×10^{-8}/sec. Most of the micrographs presented in their paper show cracks at both grain and twin boundaries.

The purpose of this report is to show and characterize where possible the transition from grain- to twin-boundary cracking in type 304 stainless steel aged at 649°C (1200°F) for 10,000 hr followed by constant-load creep testing at 593°C (1100°F). Conditions other than thermal aging that produce twin boundary cavitation are also presented. The tensile and creep properties of the specimens containing twin-boundary cavities at rupture are also included.

EXPERIMENTAL DETAILS

Two of the 20 heats of type 304 stainless steel from an ongoing mechanical properties program at Oak Ridge National Laboratory have been used here to show twin-boundary cavitation. These heats were numbered R22926 and 346845 and abbreviated to 926 and 845, respectively. The chemical analysis, vendor, and grain size of these heats are summarized in Table 1. The details of tensile and creep properties of these heats are available in other publications.[8,9]

The blocks of these heats were given the following heat treatments:

1. as received (mill annealed) and aged in air for 10,000 hr at 482, 593, and 649°C (900, 1100, and 1200°F);

---

[6] D. S. Kemsley, "Crack Paths in Fatigued Copper," *J. Inst. Metals* 85: 420–21 (1956–57).

[7] D. J. Michel, H. Nahm, and J. Moteff, "Deformation Induced Twin Boundary Crack Formation in Type 304 Stainless Steel," *Mater. Sci. Eng.* 11: 97–102 (1973).

[8] H. E. McCoy, *Tensile and Creep Properties of Several Heats of Type 304 Stainless Steel*, ORNL-TM-4709 (November 1974).

[9] V. K. Sikka, H. E. McCoy, M. K. Booker, and C. R. Brinkman, "Heat-to-Heat Variation in Creep Properties of Types 304 and 316 Stainless Steels," presented at the 2nd National Congress on Pressure Vessels and Piping, 1975 ASME Summer Meeting, June 23–27, 1975.

Table 1. Chemical Analysis of Type 304 Stainless Steel Plate Studied in This Investigation

	Heat	
	R22926	346845
Heat Symbol	926	845
Vendor	USS	Allegheny Ludlum
Thickness, in. (mm)	2(51)	2.75(70)
Grain Size[a] (intercept)		
As Received, ASTM (μm)	3.6(90)	3.8(84)
Reannealed,[b] ASTM (μm)	3.5(94)	4.0(78)
Chemical Element, %		
Carbon	0.053	0.057
Nitrogen	0.041	(0.024)
Phosphorus	0.020	0.023
Boron		0.0002
Oxygen	0.0084	0.0092
Hydrogen	0.0007	0.0013
Nickel	9.79	9.28
Manganese	1.16	0.92
Chromium	19.0	18.40
Silicon	0.68	0.53
Molybdenum	0.10	0.10
Sulfur	0.025	0.006
Niobium	0.0180	0.010
Vanadium	0.0500	0.050
Titanium	0.0100	0.008
Tantalum	0.0010	0.0005
Tungsten	0.030	0.007
Copper	0.070	0.11
Cobalt	0.050	0.07
Lead	0.010	0.01
Tin	0.02	0.01

[a]Method of Hillard, J. E., "Estimating Grain Size by the Intercept Method," *Metal Progr.* 85(5): 90–102 (May 1964). Grain size intercept excludes twin boundaries.

[b]Reannealed for 0.5 hr at 1065°C (1950°F).

2. as received and aged for 24 hr at 816°C (1500°F);
3. as received and reannealed (laboratory annealed) for 0.5 hr at 1065°C (1950°F) followed by air cooling.

Heat treatments 2 and 3 were performed in an argon atmosphere. Tensile and creep tests on unaged and aged specimens were performed at 593°C (1100°F). The tensile test strain rate was 0.04/min, whereas all creep tests were performed at a stress of 207 MPa (30 psi). Details of the aged specimens are reported elsewhere.[10]

The creep-tested specimens were examined by optical and transmission electron microscopy. The following abbreviations are used on illustrations in this report.

A 240	as-received (mill-annealed) condition, corresponding to ASME specification SA-240,
4K, 10K, etc.	refer to aging times of 4000, 10,000 hr, etc,
482, 593, 649, and 816	aging temperature in °C.

RESULTS

Mechanical Properties

Tensile and creep results on aged heat 926 of type 304 stainless steel are presented in Tables 2 and 3. The influence of aging temperature for an aging time of 10,000 hr on the stress-strain curves at 593°C (1100°F) for this heat is shown in Fig. 1. Serrations observed in load-displacement curves have not been included in the tensile curves of Fig. 1. Reannealing of the as-received material decreased yield and ultimate tensile strengths, whereas it increased the uniform and total elongations and reduction of area. Quantitative relations showing the influence of reannealing on tensile and creep properties are reported elsewhere.[11]

Bar charts showing the influence of aging time and temperature on tensile properties are presented in Fig. 2. Besides the small changes observed in yield and tensile strengths, the most noticeable influence of thermal aging was to reduce ductility at both room temperature and 593°C (1100°F).

The influence of long-term (10,000 hr) low-temperature and short-term (24 hr) high-temperature aging on creep curves for heat 926 is shown in

---

[10] V. K. Sikka, C. R. Brinkman, and H. E. McCoy, "Effect of Thermal Aging on Tensile and Creep Properties of Types 304 and 316 Stainless Steels," paper to be presented at Symposium on Structural Materials for Elevated Temperature Nuclear Power Generation Service, 1975 ASME Winter Meeting, Houston, Texas, Nov. 30 to Dec. 4, 1975.

[11] V. K. Sikka, R. W. Swindeman, T. L. Hebble, and M. K. Booker, "Residual Cold Work and its Influence on Tensile Properties of Types 304 and 316 Stainless Steel," submitted for presentation at 1975 Winter Meeting, American Nuclear Society, San Francisco, California, Nov. 16–21, 1975.

Table 2. Tensile Properties of Type 304 Stainless Steel Heat R22926 at a Strain Rate of 0.040/min

Condition	Treatment			Stress, ksi(MPa)		Strain, %		Reduction of Area (%)
	Time (hr)	Temperature (°C)	Temperature (°F)	Yield	Ultimate Tensile	Uniform	Total in 1 in.	
				Tested at 25°C (77°F)				
Reannealed	0.5	1065	1950	29.0(200)	87.4(603)	72.8	84.2	82.0
A240				36.1(249)	88.9(613)	68.4	82.7	80.3
A240, aged	4000	482	900	38.8(268)	85.7(591)	72.0	85.0	81.3
A240, aged	10,000	482	900	36.5(252)	86.6(597)	69.0	80.0	76.8
A240, aged	4000	593	1100	36.8(254)	87.3(602)	68.0	76.7	72.1
A240, aged	10,000	593	1100	36.8(254)	89.0(614	62.6	73.4	68.1
A240, aged	4000	649	1200	36.9(254)	88.2(608)	63.2	72.0	62.0
A240, aged	10,000	649	1200	34.5(238)	88.7(612)	59.4	69.8	69.1
				Tested at 593°C (1100°F)				
Reannealed	0.5	1065	1950	13.4(92)	50.5(348)	42.3	49.0	59.0
A240				19.1(132)	52.0(359)	39.0	45.1	71.0
A240, aged	4000	482	900	17.1(118)	52.6(363)	40.0	52.6	71.1
A240, aged	10,000	482	900	17.1(118)	52.4(361)	36.6	47.8	69.2
A240, aged	4000	593	1100	18.5(128)	50.9(351)	36.0	42.8	62.7
A240, aged	10,000	593	1100	20.6(142)	51.8(357)	27.6	41.2	64.1
A240, aged	4000	649	1200	20.3(140)	49.3(340)	28.8	40.6	62.9
A240, aged	10,000	649	1200	20.7(143)	49.9(344)	24.6	38.0	58.8

Table 3. Creep Properties of Aged Heat 926 of Type 304 Stainless Steel at 593°C (1100°F) and 207 MPa (30 ksi)

Condition	Treatment			Loading Strain	Time to Rupture t_r	Minimum Creep Rate $\dot{\varepsilon}_m$	Rupture Strain ε_r	Reduction of Area RA
	Time (hr)	Temperature (°C)	Temperature (°F)	(%)	(hr)	(%/hr)	(%)	(%)
Reannealed	0.5	1065	1950	7.60	2580.2	2.025×10^{-3}	28.0	31.67
As received				4.39	3074.3	1.800×10^{-3}	22.5	38.99
As received, aged	10,000	482	900	4.42	3249.5	1.975×10^{-3}	26.20	31.37
As received, aged	10,000	593	1100	2.10	930.8	2.85×10^{-3}	51.23	54.9
As received, aged	10,000	649	1200	2.83	780.6	3.5×10^{-3}	64.77	52.9
As received, aged	24	816	1500	5.77	1478.6	1.04×10^{-3}	36.1	44.5

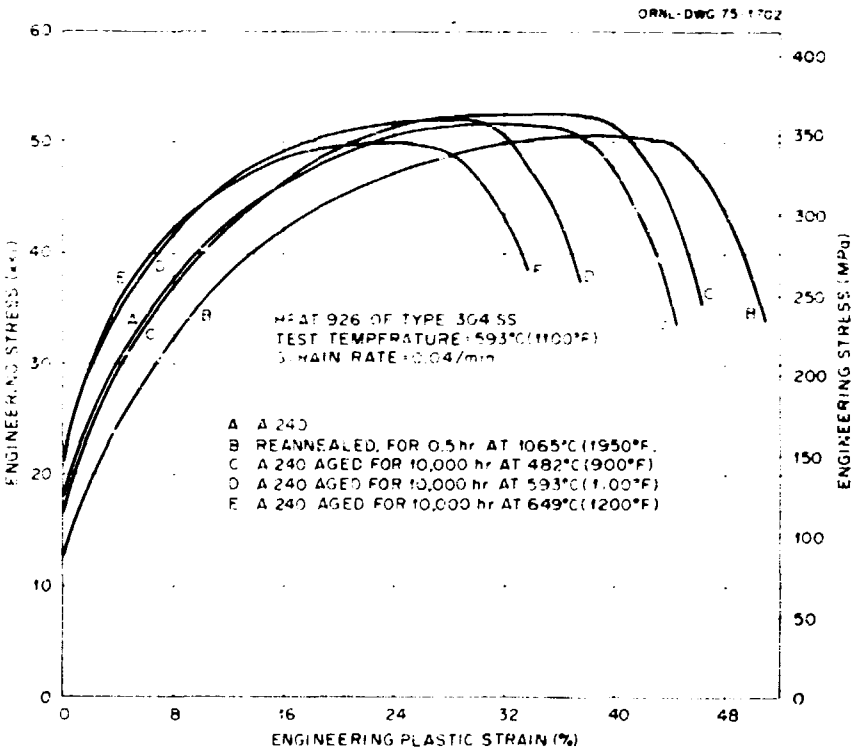

Fig. 1. Stress-Strain Curves for Heat 926 of Type 304 Stainless Steel at 593°C (1100°F) After Aging for 10,000 hr at Several Temperatures.

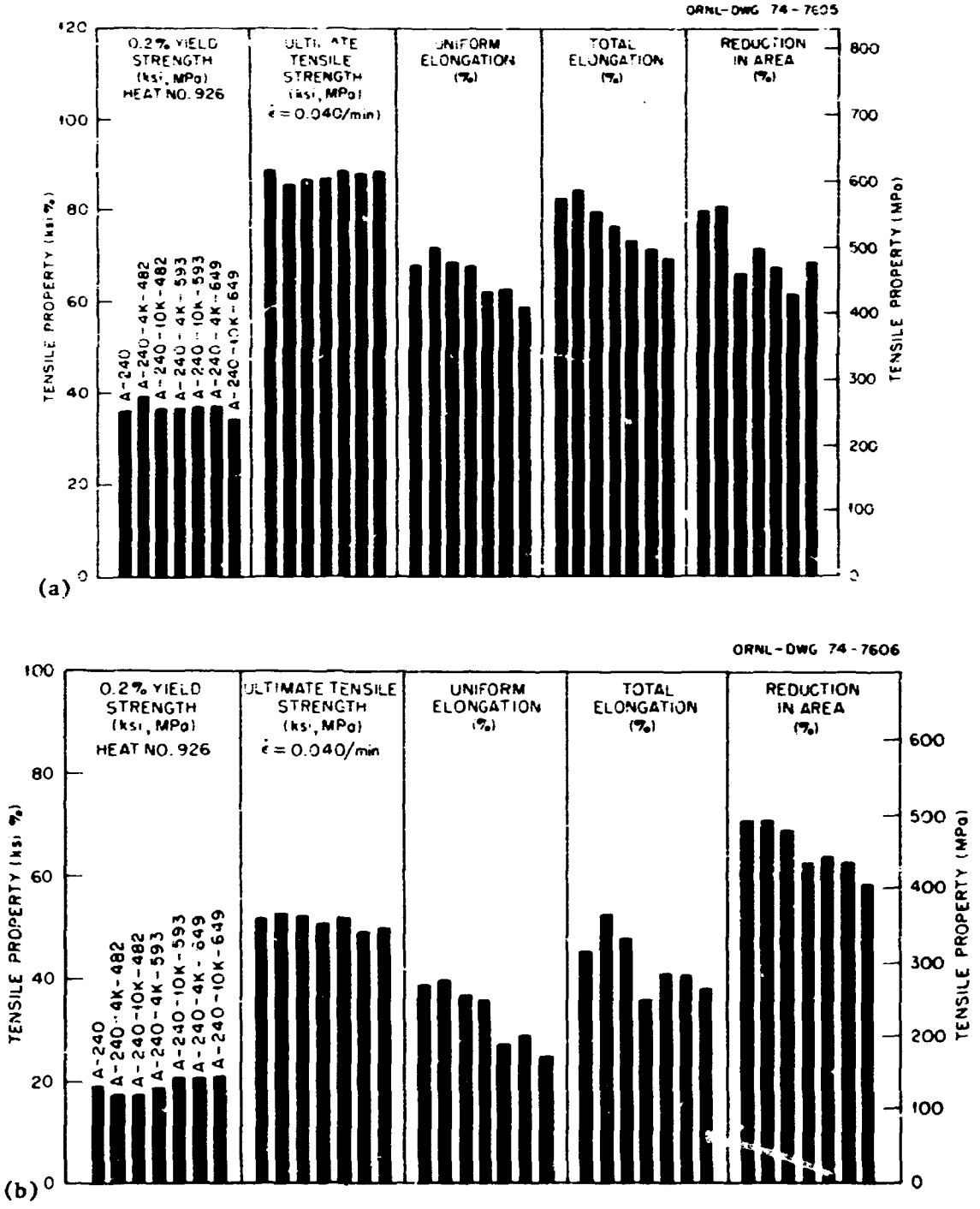

Fig. 2. Effect of Aging on Tensile Properties of Heat R22926 Aged in the As-Received Condition. (a) Room temperature, and (b) 593°C (1100°F).

Figs. 3 and 4, respectively. The following are some general observations from these figures:

1. Reannealing material in the as-received condition increases loading strain (short-term elastic and plastic strain), rupture strain, and minimum creep rate and decreases time to rupture. See ref. 11 for more details.

2. Long-term aging at 482°C has essentially little or no influence on the creep curve, whereas aging at 593 and 649°C (1100 and 1200°F) significantly alters the creep curve. Short-term aging 24 hr at 816°C (1500°F) also changes the creep curve significantly, as seen in Fig. 4. The grain size measurement showed no real grain growth for either the specimen treated 24 hr at 816°C (1500°F) or the reannealed specimen (Table 1).

3. For a given set of creep test conditions, both long-term low-temperature (LtLT) and short-term high-temperature (StHT) aging increased the minimum creep rate and decreased the time to rupture. Bar charts showing the changes in these properties are plotted in Fig. 5. The maximum change in minimum creep rate and time to rupture occurs for an aging temperature of 649°C (1200°F). A bar chart for heat 845 is also shown in Fig. 5, and it should be noted that the trends observed for heat 926 are repeated by heat 845.

4. Loading strain decreased for LtLT, whereas it increased for StHT treatment. Bar charts showing the effect of aging treatment on rupture elongation and reduction of area for heats 926 and 845 are plotted in Fig. 6. Note that peak ductility for both heats occurs for an aging temperature of 649°C (1200°F).

Metallographic Observation

The macro- and micrographs of the unaged and aged specimens are presented in Figs. 7 through 9. The increases in rupture elongation and reduction of area are quite obvious from Fig. 7. The microstructure in Fig. 8 shows wedge-type grain boundary cavities for the unaged specimen and one aged for 10,000 hr at 482°C (900°F). Note that wedge-type grain boundary cracks in Fig. 8(b) are consistent with the classical grain boundary sliding mechanism.[12] The microstructure in Fig. 9 shows annealing twin boundary cavitation for specimens aged for 10,000 hr at 593 and 649°C (1100 and 1200°F). A comparison of microstructures in Figs. 8 and 9 shows that the transition from grain- to twin-boundary cavitation starts for an aging temperature of 593°C (1100°F). Furthermore, this transition in cavitation mode is associated with a large reduction in time to rupture and a large increase in rupture elongation and reduction of area, as seen in Figs. 5 and 6. The twin-boundary cavitation in Fig. 9 is associated with extensive grain matrix (intragranular) deformation, as indicated by elongated grains, whereas grain boundary cavitation in Fig. 8 is associated with relatively little grain matrix deformation.

---

[12] F. Garofalo, *Fundamentals of Creep and Creep-Rupture in Metals*, Macmillan, New York, 1965.

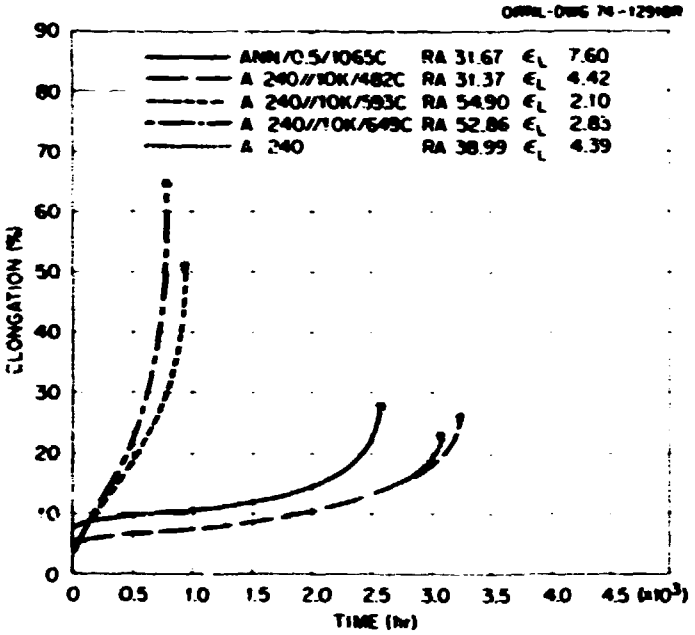

Fig. 3. Effect of Aging Temperature on Creep Curves for Heat 926 of Type 304 Stainless Steel. Creep tests were performed at 593°C (1100°F) and 207 MPa (30 ksi).

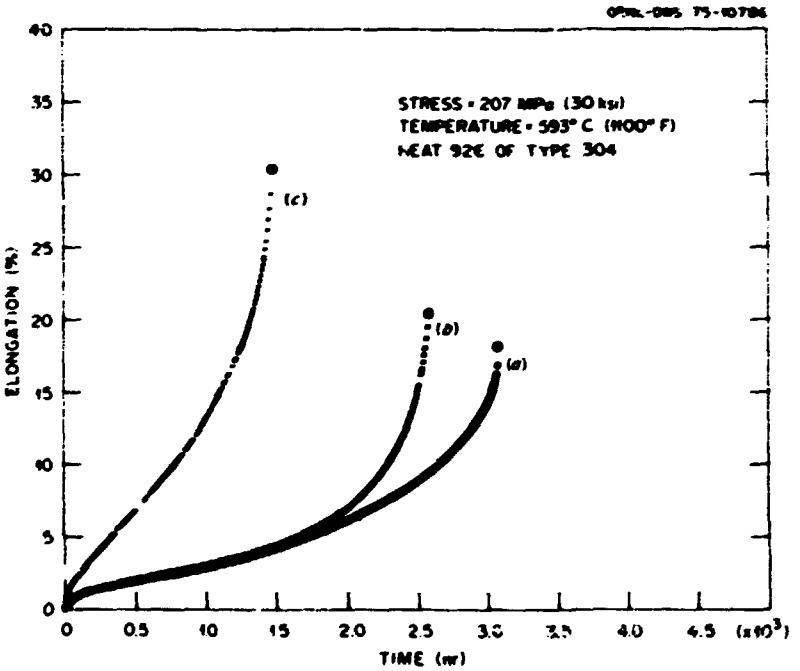

Fig. 4. Influence of Short-Term High-Temperature Aging on Creep Curves for Heat 926 of Type 304 Stainless Steel. Creep tests were performed at 593°C (1100°F) and 207 MPa (30 ksi).

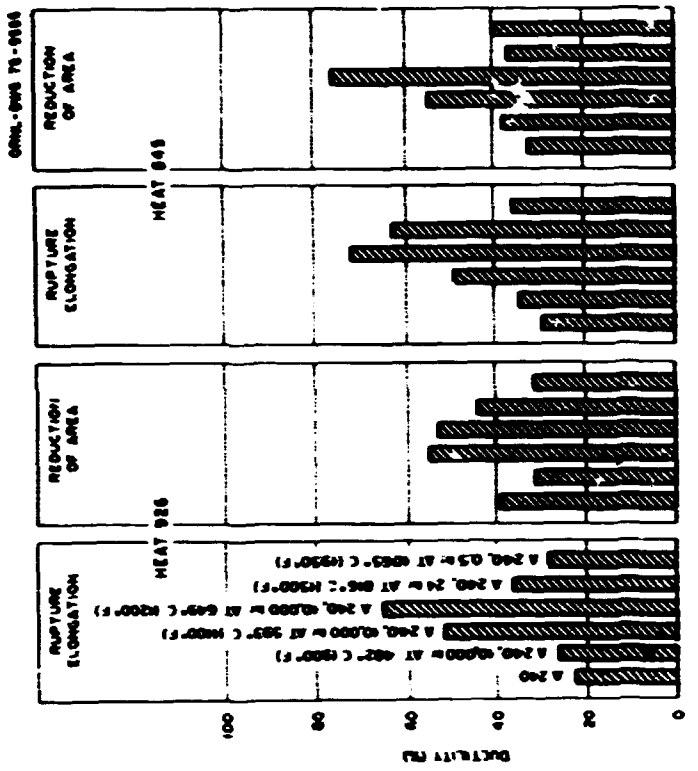

Fig. 6. Influence of Aging Treatment on Rupture Elongation and Reduction of Area for Heats 926 and 845 of Type 304 Stainless Steel. Creep tests were performed at 593°C (1100°F) and 207 MPa (30 ksi).

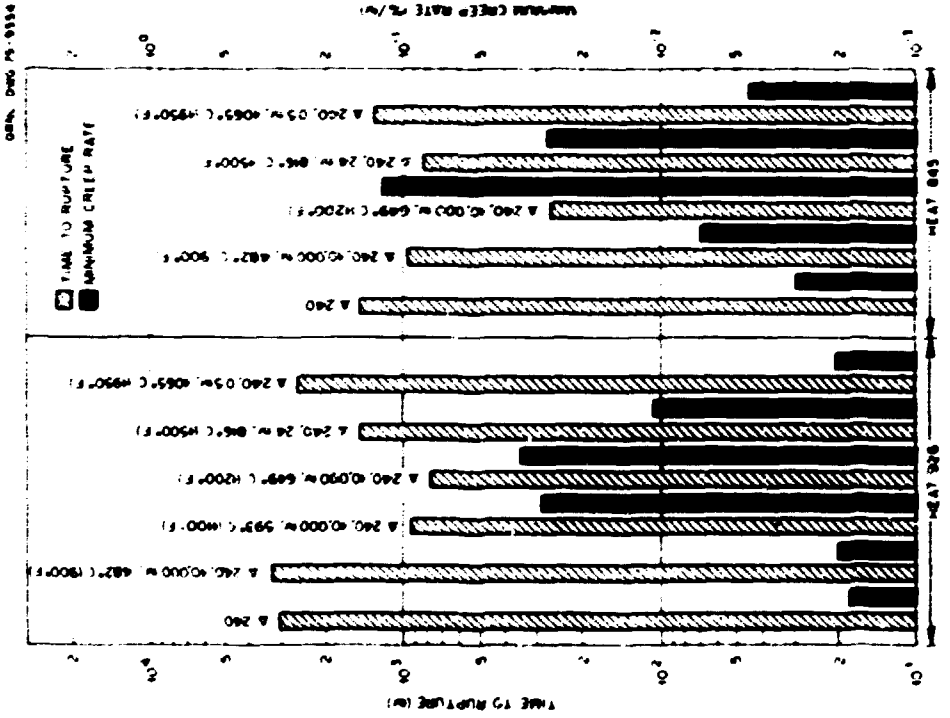

Fig. 5. Influence of Aging Treatment Time and Temperature on Time to Rupture and Minimum Creep Rate of Heats 926 and 845 of Type 304 Stainless Steel Tested at 593°C (1100°F) and 207 MPa (30 ksi).

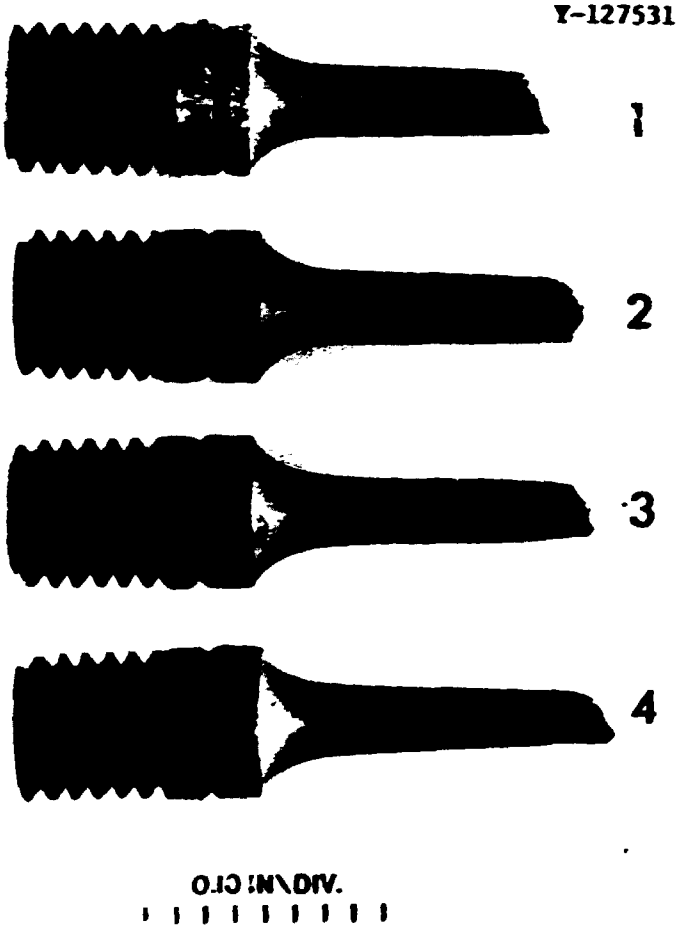

Fig. 7. Ruptured Creep Specimens of Heat 926 of Type 304 Stainless Steel Tested at 593°C (1100°F) and 207 MPa (30 ksi). Specimens 1 through 4 are as received and as received-and-aged for 10,000 hr at 482, 593, and 649°C (900, 1100, and 1200°F), respectively. Note the increase in ductility on aging.

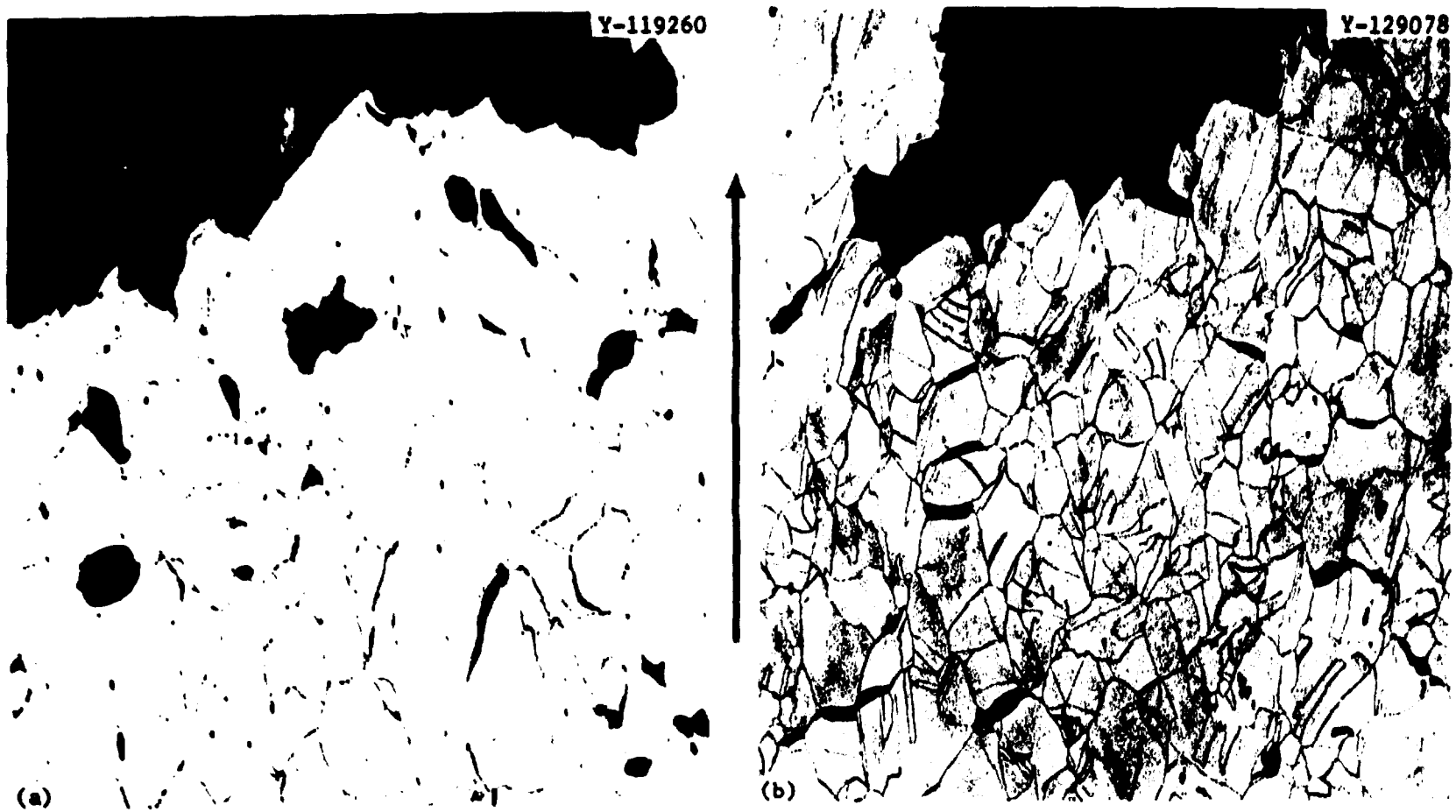

Fig. 8. Microstructure of the Fracture Ends of Creep Specimens of Heat 926 of Type 304 Stainless Steel Tested at 593°C (1100°F) and 207 MPa (30 ksi). 100×. Arrow indicates direction of applied stress. (a) Annealed and creep tested. (b) Aged at 482°C (900°F) for 10,000 hr. Note grain boundary cavitation.

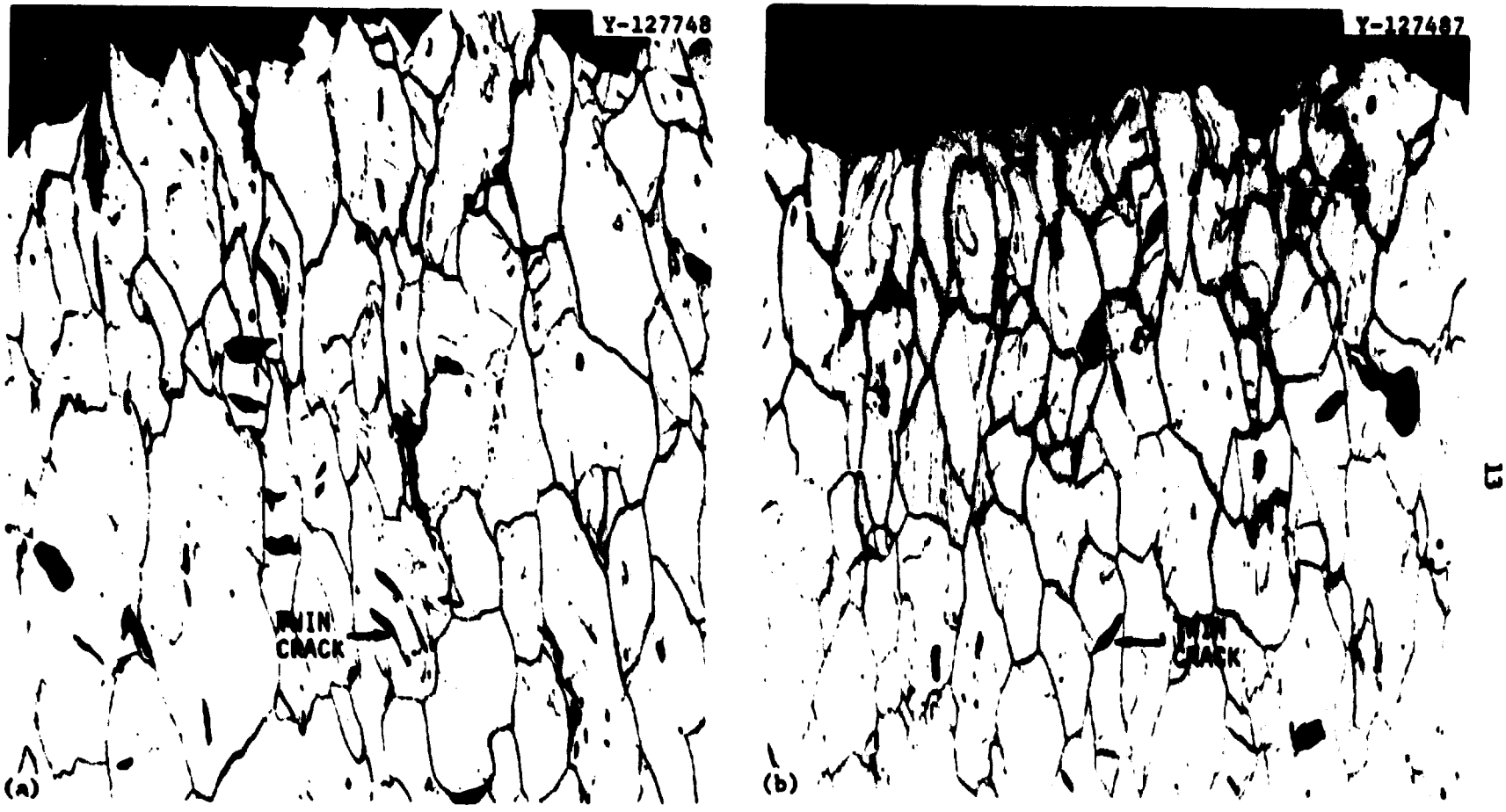

Fig. 9. Microstructure of the Fracture Ends of Creep Specimens of Heat 926 of Type 304 Stainless Steel Tested at 593°C (1100°F) and 207 MPa (30 ksi). 100×. Arrow indicates the direction of applied stress. (a) Aged at 593°C (1100°F) for 10,000 hr. (b) Aged at 649°C (1200°F) for 10,000 hr. Note the twin boundary cracking in both micrographs.

The specimen aged for 10,000 hr at 649°C (1200°F) was the first in which twin boundary cavitation has been observed and thus was examined in great detail. Figure 10 clearly shows orientation of the twin boundary cavities with respect to the stress axis in additional micrographs of the above specimen. Figure 11(a) shows a transverse twin boundary crack, whereas Fig. 11(b) shows the initiation of a surface crack along the twin boundary. High-magnification micrographs of twin boundary cracks are presented in Fig. 12. The possible nucleation of the twin boundary crack at the junction of incoherent and coherent parts of the twin is shown in Fig. 12(a). Figure 12(b) shows the propagation of the cavity nucleated at the junction of incoherent and coherent twins, along the coherent part of the twin. Figure 13 illustrates further the interesting features of twin boundary cracking. A multiple twin cracking is shown in Fig. 13(a), whereas the disappearance of an incoherent twin in the twin crack is illustrated in Fig. 13(b).

Propagation of the twin boundary crack from one grain to a twin in another grain is shown in Fig. 14. Note that the crack crosses from one grain to another without opening the grain boundary. This behavior suggests that the fracture of the specimen might have resulted from interlinking of twin boundary cracks.

The creep specimen aged for 10,000 hr at 649°C (1200°F) and tested at 593°C (1100°F) and 207 MPa (30 ksi) was also examined in a scanning electron microscope. A typical set of scanning electron micrographs is presented in Fig. 15. Note that both cracks shown are along those annealing twins that contain a small or large incoherent step. The more significant observation from Fig. 15 is a difference between the precipitates at the grain and twin boundaries. The grain boundaries contain a coarse continuous precipitate, as opposed to a fine discontinuous precipitate at the twin boundaries.

The microstructure of the specimen aged for 24 hr at 816°C (1500°F) is shown in Fig. 16. Note that the creep cavities are again along the grain boundaries (more like an unaged specimen) and that its reduction of area (Fig. 6, p. 10) has approached nearer that observed for the unaged condition. For a specimen of heat 845 of type 304, treated and tested under identical conditions, creep-induced voidage was a mixture of grain- and twin-boundary cavities as seen in Fig. 17.

Thus far extensive twin-boundary cavitation observed in specimens aged for 10,000 hr at 593 and 649°C (1100 and 1200°F) and tested at 593°C (1100°F) has been mentioned. Micrographs given in Fig. 18 show twin-boundary cracking in an unaged specimen of another heat of type 304 stainless steel (heat 813) tested at 649°C (1200°F) and 193 MPa (28 ksi). More details on tensile and creep properties of heat 813 are available in a paper by Swindeman and Pugh.[13] Thus, prior aging is not a necessary condition for twin-boundary cavitation.

Specimens were also examined of type 316 stainless steel, aged for 10,000 hr at 649°C (1200°F) and tested at 593°C (1100°F) and 241 MPa (35 ksi). Typical micrographs of a specimen of this material showing

---

[13]R. W. Swindeman and C. E. Pugh, *Creep Studies on Type 304 Stainless Steel (Heat 8043813) Under Constant and Varying Loads*, ORNL-TM-4427 (June 1974).

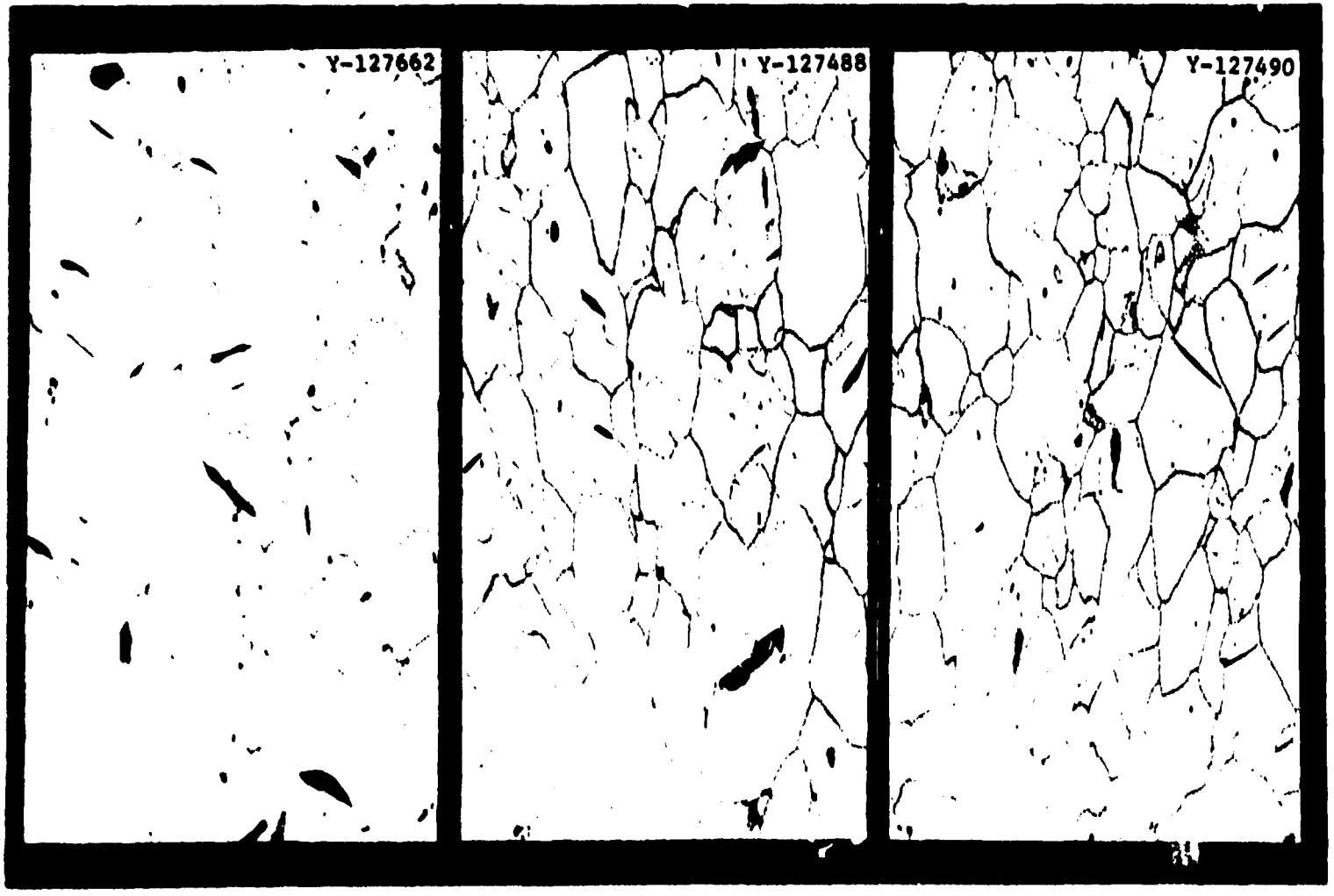

Fig. 10. Microstructure Showing Extensive Twin Boundary Cracking in a Specimen Creep Tested at 593°C (1100°F) and 207 MPa (30 ksi) for Heat 926 of Type 304 Stainless Steel, Aged at 649°C (1200°F) for 10,000 hr. 100×. Arrow indicates direction of applied stress in all three views.

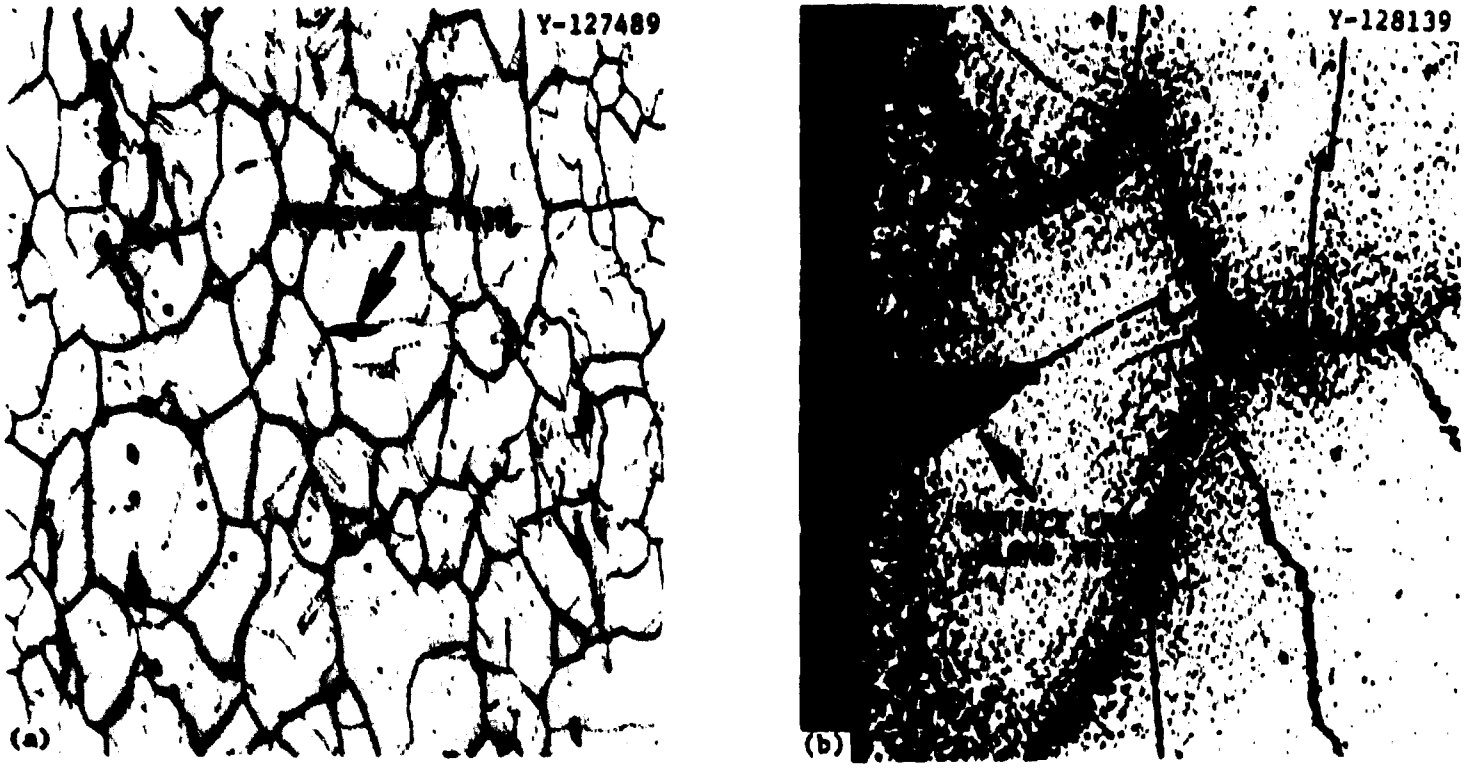

Fig. 11. Characteristic Features of Twin Boundary Cavities. (a) A transverse twin crack. 100×. (b) Surface crack propagating along the twin boundary. 1000×. Both micrographs are from creep specimens of heat 926, aged for 10,000 hr at 649°C (1200°F) and tested at 593°C (1100°F) and 207 MPa (30 ksi).

Fig. 12. Micrographs of the Creep Specimen of Heat 926 of Type 304 Stainless Steel Aged for 10,000 hr at 649°C (1200°F) and Tested at 593°C (1100°F) at 207 MPa (30 ksi). Arrow indicates direction of applied stress. 1000×. (a) Twin cavity nucleated at intersection of incoherent-coherent twin junction. (b) Twin crack propagated along the coherent twin.

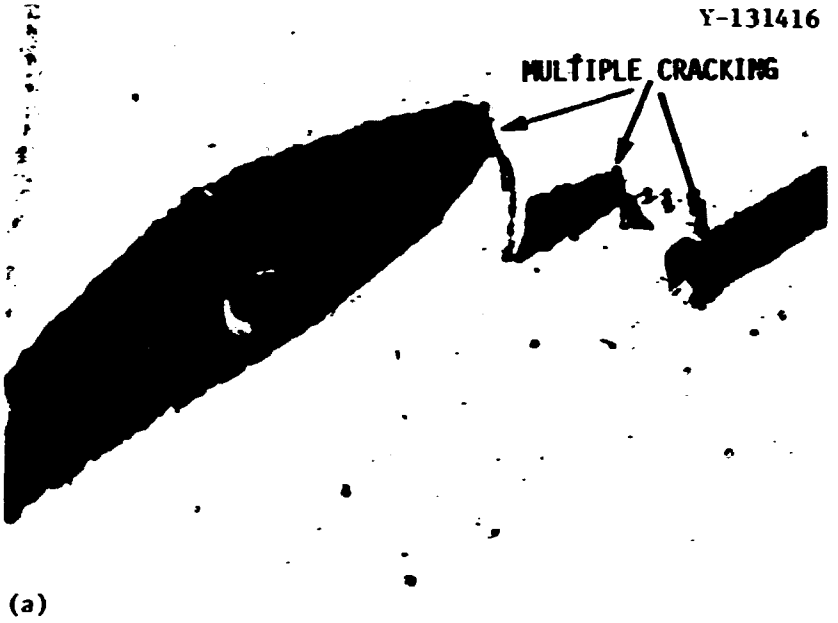

(a)

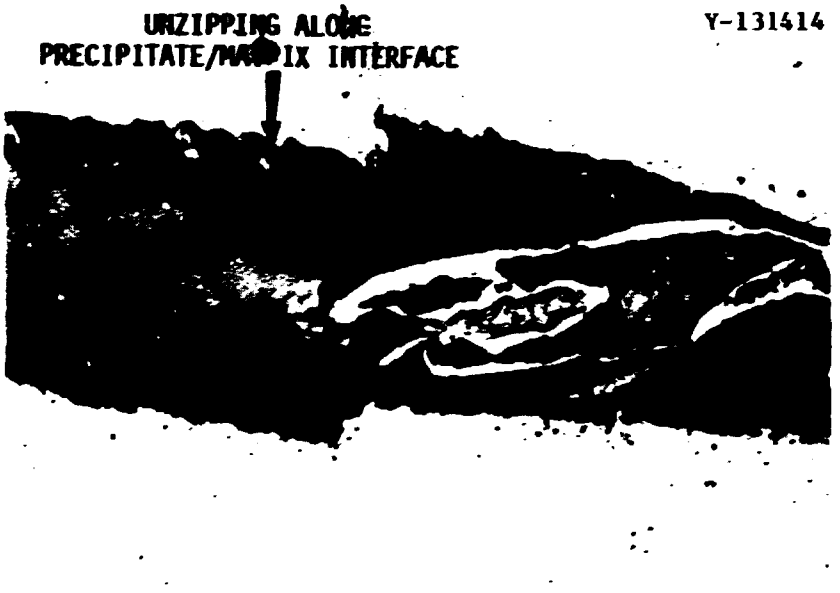

(b)

Fig. 13. The Creep Specimen of Heat 926 of Type 304 Stainless Steel Aged for 10,000 hr at 649°C (1200°F) and Tested at 593°C (1100°F) at 207 MPa (30 ksi). Arrow indicates the direction of applied stress. 1500×. (a) Multiple twin boundary cracking. (b) "Unzipping" along the precipitate-matrix interface.

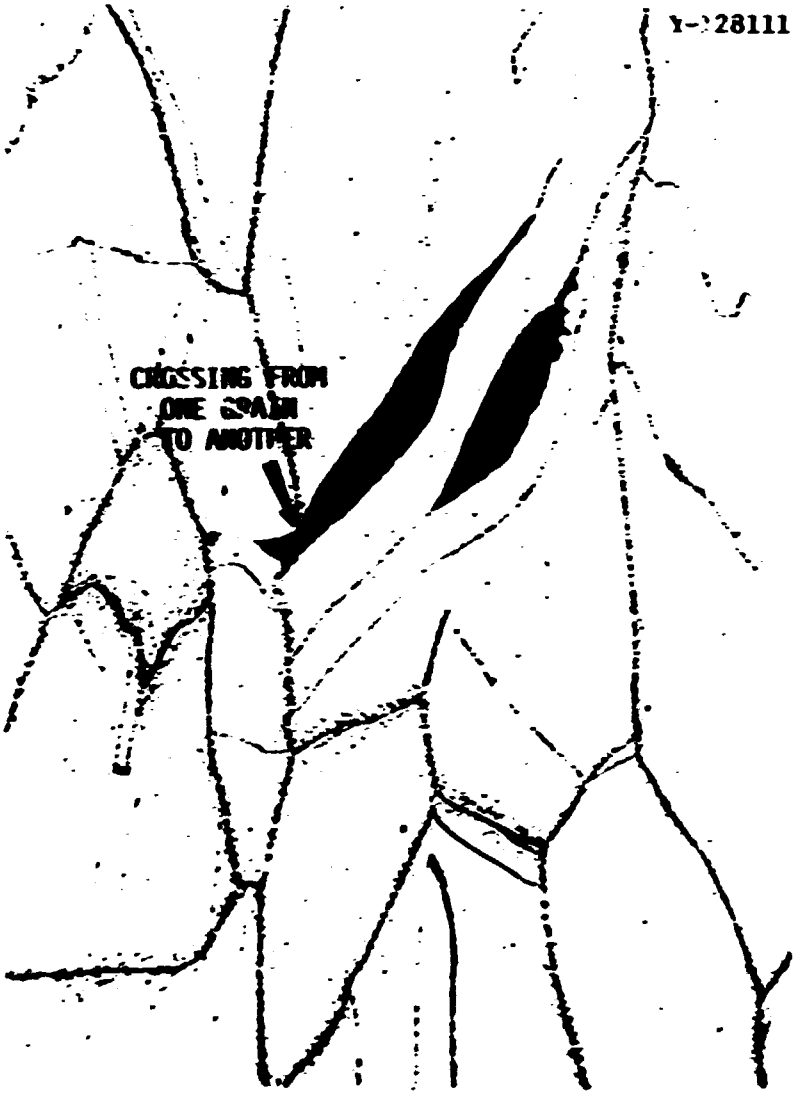

Fig. 14. Creep Specimen of Heat 926 of Type 304 Stainless Steel, Aged for 10,000 hr at 649°C (1200°F) and Tested at 207 MPa (30 ksi). Micrograph shows the propagation of a twin crack from one grain to another. Arrow indicates the direction of applied stress. 500×.

Y-130424

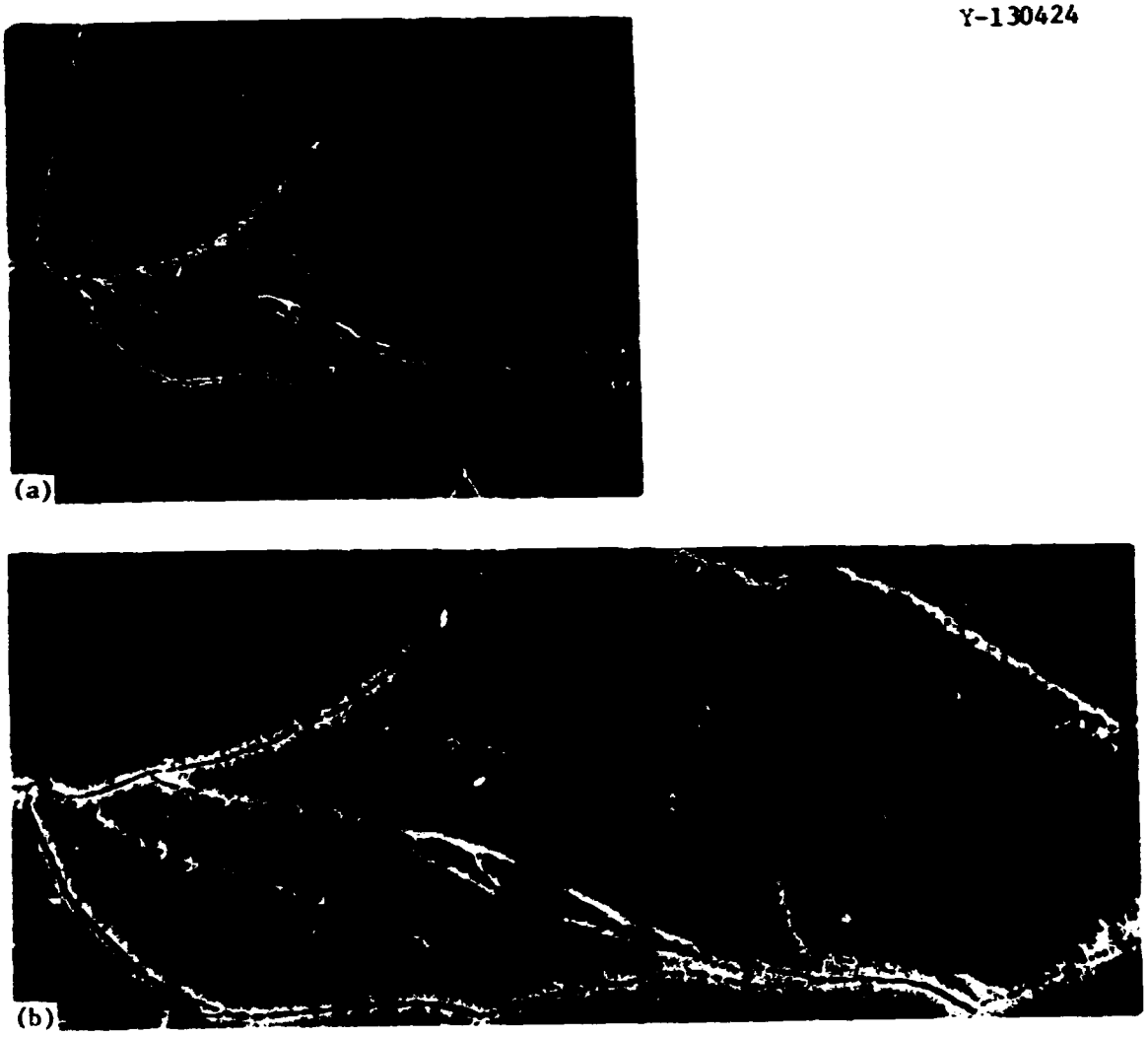

Fig. 15. Scanning Electron Micrographs from Creep Specimen of Heat 926 of Type 304 Stainless Steel, Aged for 10,000 hr at 649°C (1200°F) and Tested at 593°C (1100°F). (a) Twin cracks, 500×. (b) Twin crack stopped by incoherent segments, 1000×. (c) Difference in precipitate distribution at grain and twin boundaries, 3000×.

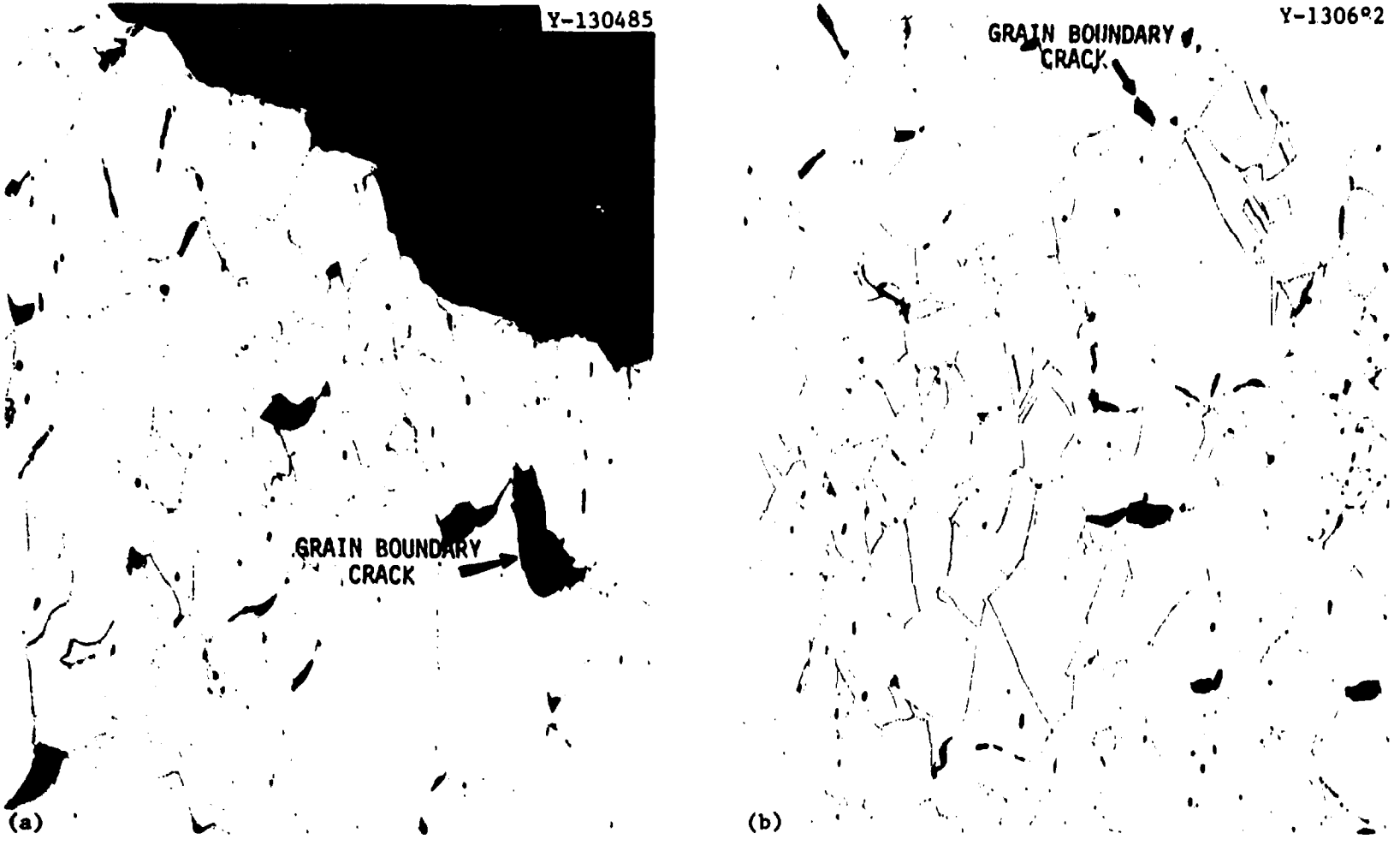

Fig. 16. Microstructure of Creep Specimen of Heat 926 of Type 304 Stainless Steel, Aged for 24 hr at 816°C (1500°F) and Tested at 593°C (1100°F) and 207 MPa (30 ksi). Arrow indicates the direction of applied stress. 100×. (a) Fracture end. (b) End away from fracture. Note the presence of primarily grain boundary cracks.

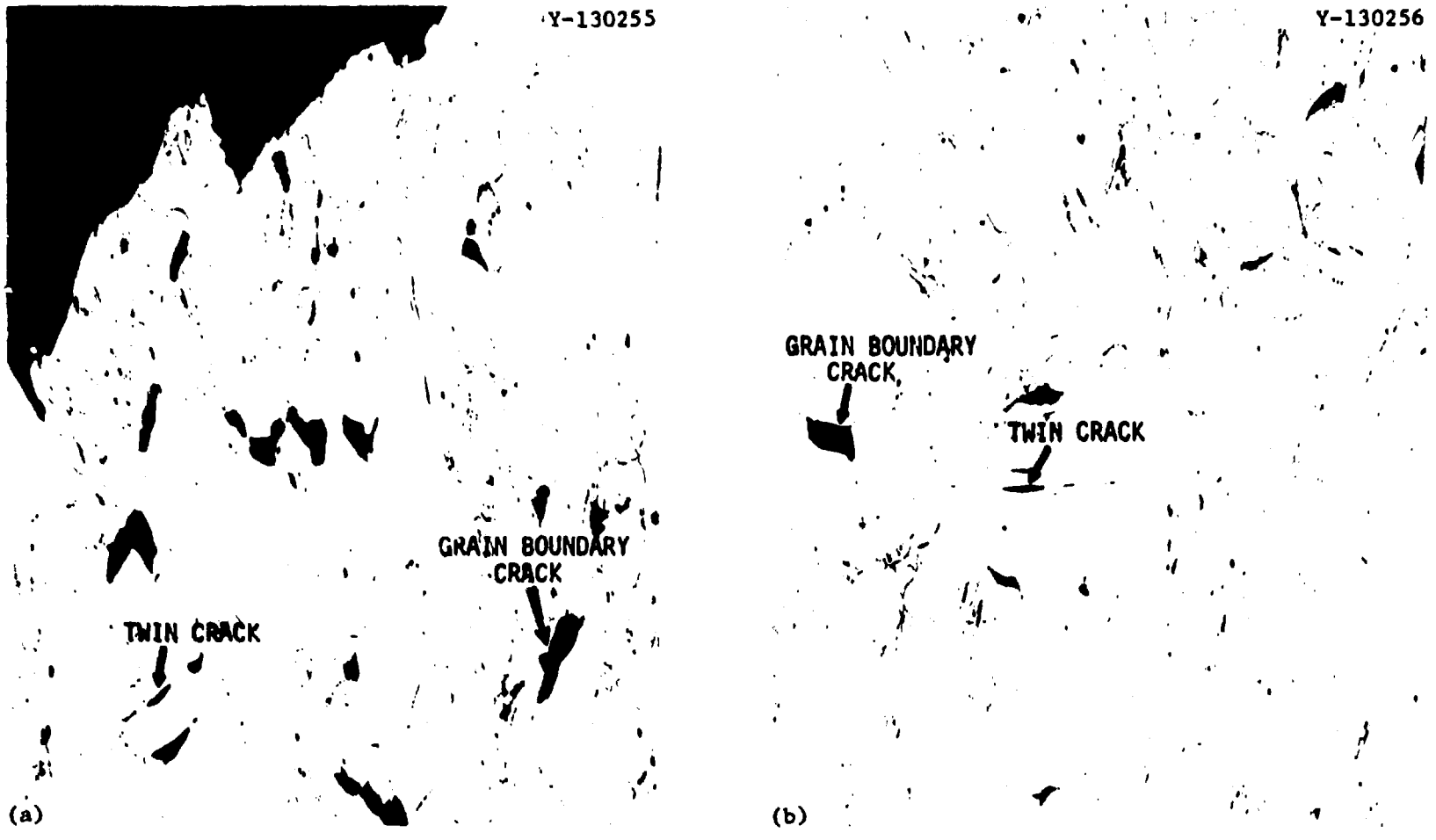

Fig. 17. Microstructure of Creep Specimen of Heat 845 of Type 304 Stainless Steel, Aged for 24 hr at 816°C (1500°F) and Tested at 593°C (1100°F) and 207 MPa (30 ksi). Arrow indicates the direction of applied stress. 100×. (a) Fracture end. (b) End away from fracture. Note the presence of twin and grain boundary cracks.

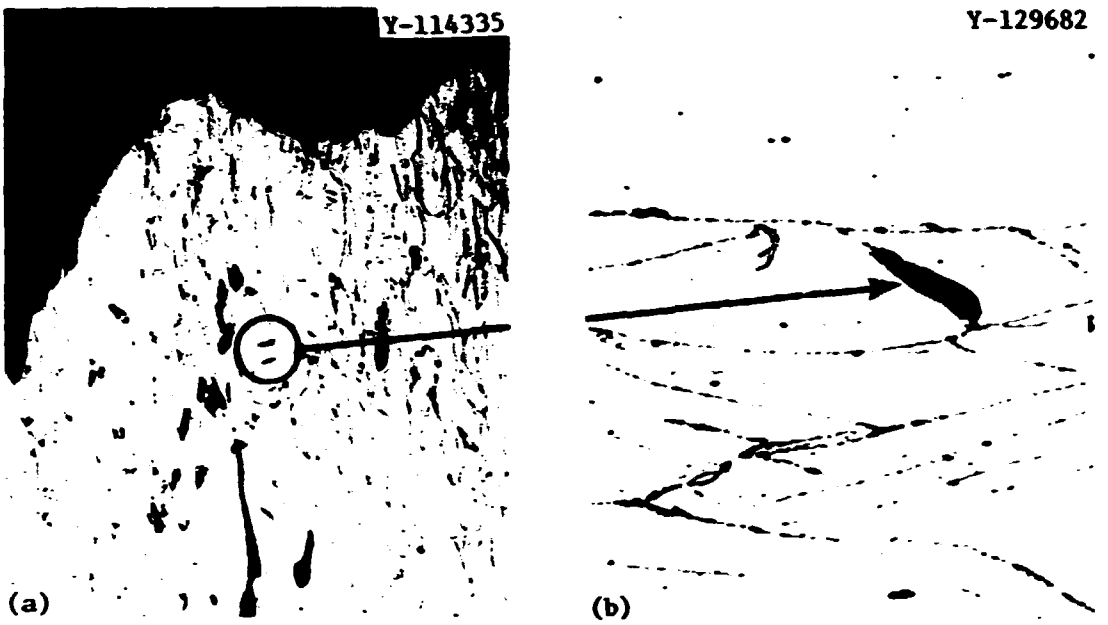

Fig. 18. Twin Boundary Cracking in Microstructure of Creep Specimen of Heat 813 of Type 304 Stainless Steel Tested at 649°C (1200°F) and 193 MPa (28 ksi). Note that this specimen was not preaged. (a) 50×. (b) 500×.

twin boundary cavities are presented in Fig. 19. Thus, twin boundary cavitation can be observed under proper conditions in both types 304 and 316 stainless steel.

Transmission electron micrographs of the unaged specimen and one aged for 10,000 hr at 649°C (1200°F) are shown in Fig. 20. The precipitate particle sizes and densities were measured from these micrographs and are summarized in Table 4. It is noted that the precipitate at the grain boundaries is coarse and continuous, whereas it is fine and discontinuous at the twin boundaries of the aged specimen. No precipitate was observed at the twin boundaries during creep testing of the unaged specimen. Furthermore, the precipitate particle size and shape at the grain boundaries where cracking occurred in the unaged specimen are similar to those of precipitate particles at the twin boundaries where cracking occurred in the aged specimen. The ORNL precipitate size data in Table 4 on unaged and aged specimens of heat 926 of type 304 stainless steel compare remarkably well with those reported by Etienne et al.[14]

High-magnification optical micrographs (1500×) for long-term low-temperature and short-term high-temperature treated specimens, tested under identical conditions, are shown in Figs. 21 and 22. The comparison

[14]E. F. Etienne, W. Dortland, and H. B. Zeedijk, "On the Capability of Austenitic Steel to Withstand Cyclic Deformation During Service at Elevated Temperature," paper presented at International Conference on Creep and Fatigue in Elevated Temperature Applications, Philadelphia, September 1973 and Sheffield, UK, April 1974.

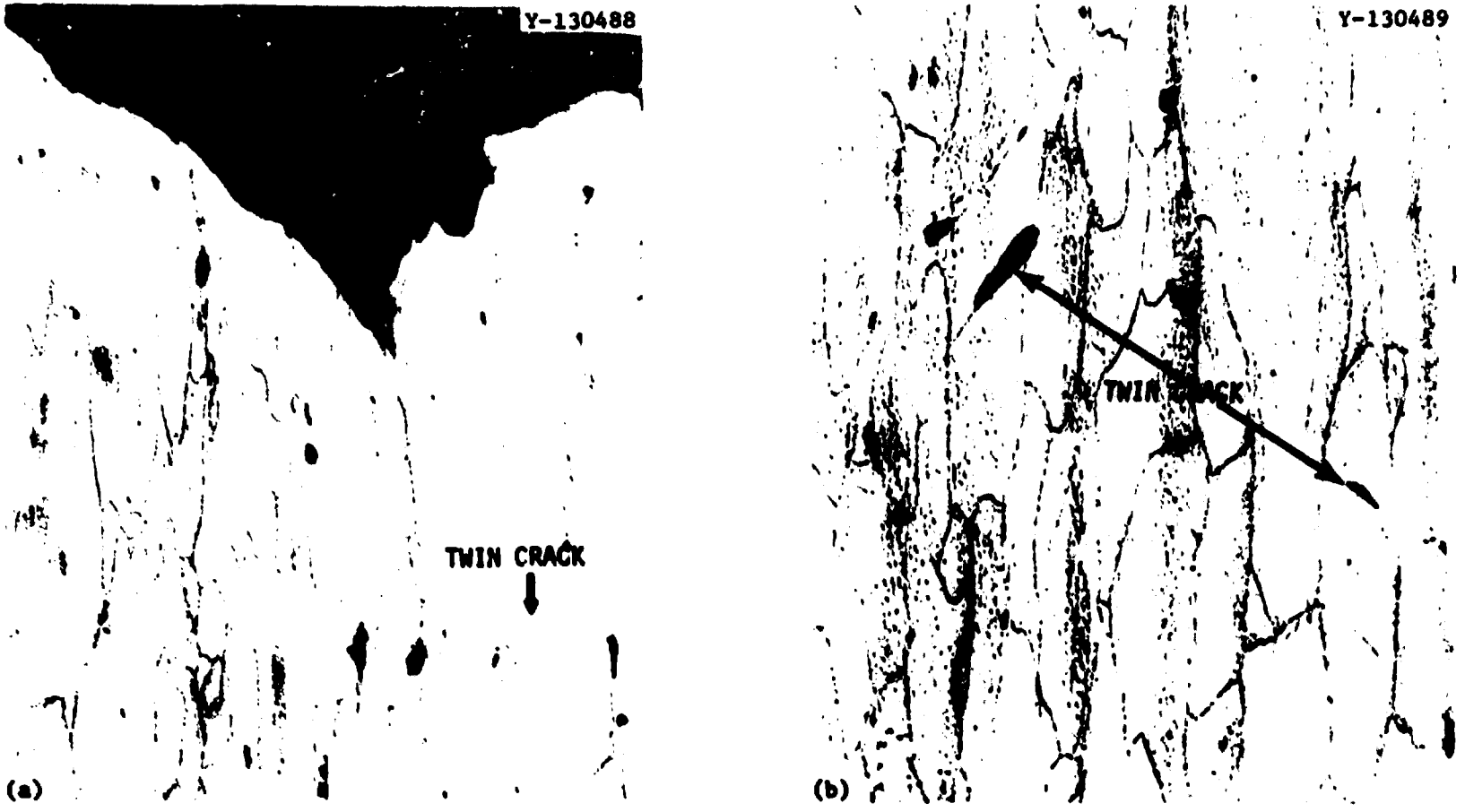

Fig. 19. Microstructure of Creep Specimen of Heat 509 of Type 316 Stainless Steel, Aged for 10,000 hr at 649°C (1200°F) and Tested at 593°C (1100°F) and 207 MPa (30 ksi). Arrow indicates the direction of applied stress. (a) Fracture end, 100×. (b) Area farther away from fracture end, 200×. Note twin boundary cracks in both micrographs.

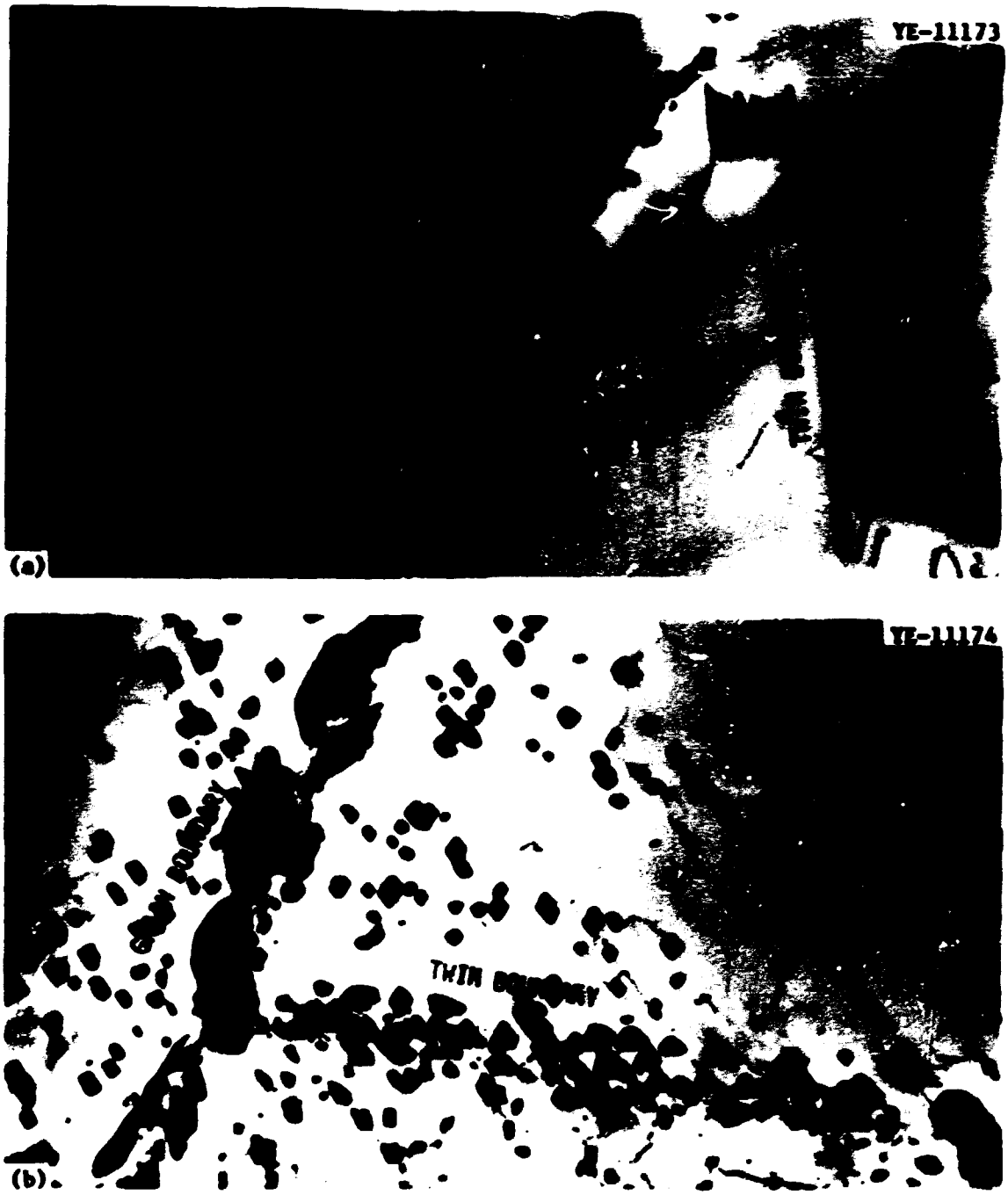

Fig. 20. Electron Micrographs from Buttonheads of Creep Specimens of Heat 926 of Type 304 Stainless Steel. (a) Annealed, tested 2580 hr at 593°C (1100°F). (b) Aged for 10,000 hr at 649°C (1200°F), tested 780 hr at 593°C (1100°F). Note the difference in precipitate at twin and grain boundaries.

Table 4. Summary of Precipitate Data for Heat 926 of Type 304 Stainless Steel

Temperature, °C(°F)		Time, hr		Precipitate Character at Various Locations						Reference
				Matrix		Grain Boundary		Twin Boundary		
Aging	Test	Aging	Test	Size (μm)	Density (cm^{-3})	Size (μm)	Density (cm^{-1})	Size (μm)	Density	
	593(1100)		2,580	0.069	5.7×10^{12}	0.35	4.8×10^{4}	a	a	ORNL
	593(1100)		~2,580	0.020	b	~0.30	b	b	b	c
649(1200)	593(1100)	10,000	780	0.130	4.3×10^{13}	1.26	1.15×10^{4}	0.20	b	ORNL
	649(1200)		~11,000	0.05–0.10	b	1.0	b	b	b	c

[a]None observed.

[b]Not measured or reported.

[c]C. F. Etienne, W. Dortland, and H. B. Zeedijk, "On the Capability of Austenitic Stainless Steel to Withstand Cyclic Deformation During Service at Elevated Temperature," Paper Presented at the International Conference on Creep and Fatigue in Elevated Temperature Applications, Philadelphia, September 1973, and Sheffield UK, April 1974.

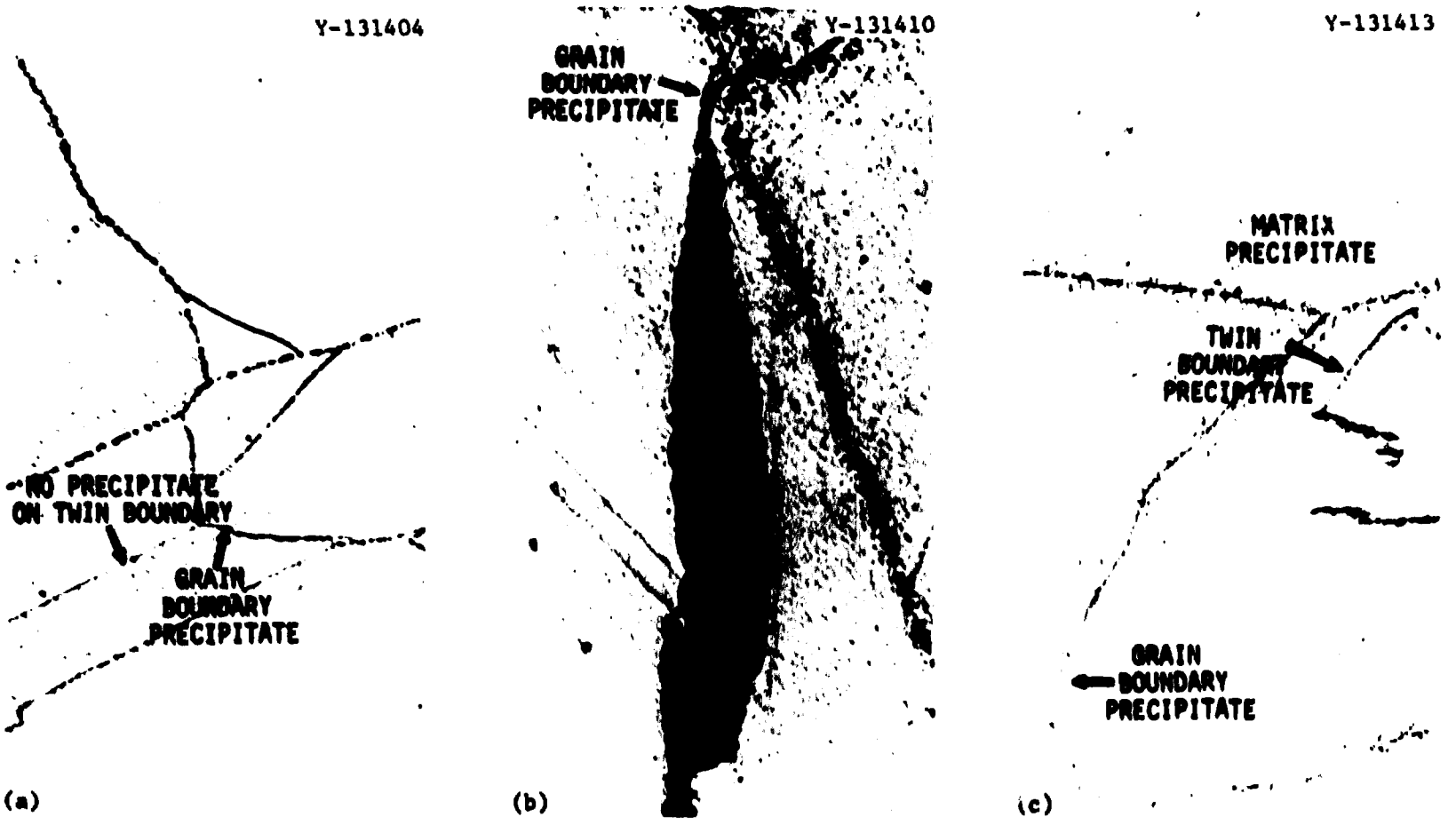

Fig. 21. Micrographs of Creep Specimens of Heat 926 of Type 304 Stainless Steel Aged for 10,000 hr at (a) 482°C (900°F), (b) 593°C (1100°F), and (c) 649°C (1200°F). Note the difference in precipitates between the three specimens and compare with Fig. 22.

Fig. 22. Creep Specimen of Heat 926 of Type 304 Stainless Steel Aged 24 hr at 816°C (1500°F) and Tested at 593°C (1100°F) and 207 MPa (30 ksi). 1500×. Note the large precipitate particles at the twin and grain boundaries and their absence from the matrix. Compare with precipitate particle size and location in Fig. 21.

between these figures shows that StHT treatment yielded precipitate only at the grain boundaries, whereas LtLT treatment produced precipitate in the matrix as well as at the grain boundaries.

DISCUSSION

Long-term low-temperature aging for 4000 to 10,000 hr at 482, 593, and 649°C (900, 1100, and 1200°F) increased the yield stress. This increase is also reflected by a decrease in loading strain during the creep test. Furthermore, the flow stress is higher for the aged material over the entire range of the stress-strain curve from the proportional limit to near the ultimate tensile strength. At strain levels coinciding with and beyond the ultimate tensile strength the flow stress was lower as seen in Fig. 1 (p. 6). Short-term high-temperature treatment resulted in a decrease in yield strength (determined from the loading curve during the creep test), which is also reflected by an increase in loading strain.

The changes produced in yield strength on thermal aging were not reflected by the creep-rupture properties. For example, increase in yield strength accompanied a decrease in time to rupture. On the other hand, changes produced in ultimate tensile strength were reflected in corresponding changes in creep strength. For example, a decrease in ultimate tensile strength resulted in an increase in minimum creep rate and decrease in time to rupture. The above observations are consistent with the recent development[15,16] of a relation between elevated-temperature ultimate tensile strength and time to rupture or creep-rupture strength

$$S_R^t = \alpha \exp(\beta S_u^r) \quad , \tag{1}$$

where

S_R^t = creep-rupture strength,

S_u^r = ultimate tensile strength at the creep test temperature and a fixed tensile strain rate r measured on specimens that had not been creep tested,

α, β = material constants.

---

[15] V. K. Sikka, H. E. McCoy, M. K. Booker, and C. R. Brinkman, "Heat-to-Heat Variation in Creep Properties of Types 304 and 316 Stainless Steels," presented at the 2nd National Congress on Pressure Vessels and Piping, 1975 ASME Summer Meeting, June 23–27, 1975.

[16] V. K. Sikka and C. R. Brinkman, "Relation Between Short- and Long-Term Elevated-Temperature Properties of Several Austenitic Stainless Steels," submitted for publication.

Constants α and β are essentially the same for both unaged and aged material.[16,17] Thus, a decrease in ultimate tensile strength on thermal aging is expected from Eq. (1) to result in a decrease in time to rupture or creep-rupture strength and is consistent with the observed results.

One important difference between the unaged and aged specimens was that for the unaged specimen the precipitate particles nucleated and grew during the creep test, whereas for the aged specimens the precipitate was present before creep and might have grown some during the creep test. The matrix precipitate in the aged specimen results in precipitation hardening, as evidenced by the increase in yield strength [see Fig. 2(b)] and decrease in the loading strain (Fig. 3). For the unaged specimen, the grain boundary precipitate becomes apparent[18] approximately 10 hr after the start of a creep test at 593°C (1100°F) and 207 MPa (30 ksi). Second-stage creep for this test starts at approximately 350 hr. It therefore follows that the nucleation and growth of matrix precipitate particles must be occurring during the second-stage creep of the unaged specimen.

Thermal aging of austenitic stainless steels produces precipitates in the matrix and at the grain-boundaries, as seen in Figs. 21 and 22, and there is no model available at present to explain the influence of such a combination of precipitates on the creep properties. Ansell and Weertman[19] developed a dislocation creep model for the effect of dispersed particles on steady-state creep. The basis of the theory involves the climb of mobile dislocations over particles and their annihilation by dislocations of opposite sign on neighboring parallel slip planes. An attempt is made here to see if that model can account for the observed behavior of aged type 304 stainless steel. According to the model, minimum creep rate is given by

$$\dot{\varepsilon}_m = 6\tau^4 D_g \lambda^2 / dG^3 kT \ , \qquad (2)$$

---

[17] V. K. Sikka, C. R. Brinkman, and H. E. McCoy, "Effect of Thermal Aging on Tensile and Creep Properties of Types 304 and 316 Stainless Steels," paper to be presented at Symposium on Structural Materials for Elevated Temperature Nuclear Power Generation Service, 1975 ASME Winter Meeting, Houston, Texas, Nov. 30 to Dec. 4, 1975.

[18] E. F. Etienne, W. Dortland, and H. B. Zeedijk, "On the Capability of Austenitic Steel to Withstand Cyclic Deformation During Service at Elevated Temperature," paper presented at International Conference on Creep and Fatigue in Elevated Temperature Applications, Philadelphia, September 1973 and Sheffield, UK, April 1974.

[19] G. S. Ansell and J. Weertman, *Trans. AIME* 215: 838–43 (1959), as cited by F. Garofalo, *Fundamentals of Creep and Creep-Rupture in Metals*, Macmillan, New York, 1965.

where τ = applied shear stress,

D_s = self-diffusion coefficient of the matrix atom,

λ = interparticle spacing for precipitate in the matrix

d = particle diameter,

G = shear modulus, and

k = Boltzmann constant.

For identical creep test conditions, neglecting a small change in D_s due to the depletion of approximately 1% Cr from matrix, the ratio of the minimum creep rates in aged and unaged conditions can be expressed as:

$$\frac{\dot{\varepsilon}_m(\text{aged})}{\dot{\varepsilon}_m(\text{unaged})} = \frac{\lambda_A^2 \dot{\varepsilon}_{UA}}{d_A \lambda_{UA}^2} \quad . \tag{3}$$

The interparticle spacing can be related to the particle size and density by the relation

$$\lambda = 1/\sqrt{Nd} \quad , \tag{4}$$

where N = number of particles per unit volume in the matrix. Combining Eq. (4) with (3) gives:

$$\frac{\dot{\varepsilon}_m(\text{aged})}{\dot{\varepsilon}_m(\text{unaged})} = \frac{N_{UA} d_{UA}^2}{N_A d_A^2} \quad . \tag{5}$$

Substituting values of particle size and density from Table 4 into Eq. (5) yielded $\dot{\varepsilon}_m(\text{aged})/\dot{\varepsilon}_m(\text{unaged}) \approx 1/27$, as opposed to a value of approximately 19 observed in the present investigation. Such a large difference between theory and experimental data may be associated with the strong influence of grain-boundary precipitates, which was not considered in the Ansell and Weertman[19] theory.

Qualitatively, we expect the carbides that are nucleated and grown during second-stage creep in the unaged specimen to effectively anchor the dislocations and impede recovery.[20] Such a process would decrease the creep rate and thus increase the time to rupture. For the aged specimen carbides exist before testing. Although they increase the yield strength, they prevent the formation of dislocation cell or subgrain structure and thus may accelerate dislocation recovery and minimum creep

---

[20] I. R. McLauchlin, "The Effect of Long Aging Treatments on Steady-State Creep in 20% Cr-25% Ni, Nb-Stabilized Stainless Steel," *Metal Sci.* 8: 247–52 (1974).

rate. The above suggestions are consistent with the results of Garofalo et al.,[21] who found that prestrain followed by precipitation led to a 25-fold increase in the time to rupture.

The initiation of intergranular cavitation requires the presence of any or all of the following:[22]

1. grain-boundary sliding,
2. high intragranular flow strength,
3. nonwetting inclusions (oxides etc.) at the grain boundaries,
4. impurity segregation at grain boundaries preventing grain boundary migration,
5. brittle film formation at the grain boundaries, and
6. denudation phenomenon in alloys;

and absence of any or all of the following:

1. grain-boundary migration,
2. high cohension between the particle and matrix,
3. a phase change, and
4. recrystallization.

Garofalo[22] investigated the influence of grain boundary precipitate morphology on the intergranular cavitation of type 316 stainless steel. For the annealed condition small closely spaced carbide particles were precipitated at the grain boundaries at 593°C (1100°F). No grain boundary migration was possible under these conditions; the elongation at rupture was low and the fracture totally intergranular. The present results for heat 926 of type 304 stainless steel show small (0.35 μm) closely spaced particles (0.21 μm apart) after tests at 593°C (1100°) and 207 MPa (30 ksi). Rupture under these conditions was intergranular [see Fig. 8(a), p. 12] with a rupture total elongation of 28.0%. Thus, intergranular cavitation in heat 926 quite possibly occurred by a mechanism suggested by Garofalo for type 316 stainless steel tested under similar conditions.

Garofalo[22] pretreated type 316 stainless steel for 24 hr at 816°C (1500°F) before testing at 593°C (1100°F). This pretreatment increased rupture life and elongation. The increase in time to rupture was suggested to have resulted from the grain boundary migration due to pretreatment. The pretreatment was thought to have spheroidized the precipitate, as compared with the formation of a fine precipitate in the annealed material during testing at 593°C (1100°F). The fracture behavior of the pretreated specimen was still intergranular, but no cracks were observed along the precipitate-matrix interface. The lack of cracks along the precipitate particles was considered as the possible result of strong adherence between the matrix and the particles. In the present investigation, thermal aging for 10,000 hr at 649°C (1200°F) increased the grain boundary precipitate particle size from 0.35 to 1.26 μm and particle spacing from 0.21 to 0.87 μm. Contrary to the results of Garofalo, the time to rupture decreased by 75%, and no intergranular cavities were observed. Instead, the cavities were all along the twin boundaries (Figs.

---

[21]F. Garofalo, F. von Gemmingen, and W. F. Domis, "The Creep Behavior of an Austenitic Stainless Steel as Affected by Carbides Precipitated on Dislocations," *ASM (Amer. Soc. Metals) Trans. Quart.* 54: 430–44 (1961).

[22]F. Garofalo, *Fundamentals of Creep and Creep-Rupture in Metals*, Macmillan, New York, 1965.

9–13). The absence of grain boundary cavities may be the result of the following conditions produced by thermal aging:

1. Intragranular flow strength was lower than that of grain boundaries. The intragranular deformation, ϵ_g, was calculated by the following relation:[23]

$$\epsilon_g = \left(\frac{\ell}{w} \cdot \frac{w_0}{\ell_0}\right)^{2/3} - 1 , \qquad (6)$$

where ℓ_0/w_0 and ℓ/w are the average length-to-width ratios in the annealed and deformed specimens, respectively, ℓ being measured parallel and w transverse to the stress axis. The calculated value of ϵ_g was 75%, which compared extremely well with the true measured ductility of 75.3%, thus indicating that total deformation was all intragranular.

2. Coarse precipitates in the aged specimen might have resulted in grain-boundary migration, as observed by Garofalo[22] in pretreated type 316 stainless steel, and thus prevented or even eliminated grain boundary sliding.

3. The coarse precipitate at the grain boundaries of the aged specimen might have more cohesion with the matrix than the fine precipitate at the twin boundaries of the aged specimen and at grain boundaries of the unaged specimen. Such a possibility is suggested because cavitation was observed at the location of small precipitate particles (grain boundaries of the unaged tested specimen and twin boundaries of the aged tested specimens).

Some or all of the above-mentioned factors may be operating to prevent grain-boundary cracking.

Greenwood et al.[24] investigated the intergranular cavitation in stressed metals (copper, α-brass, and magnesium) containing annealing twins. They showed no cavities in copper and pointed out that voids do not form on twin boundaries even when the boundaries are transverse to the applied stress. The only observation where twin cracks have been reported in type 304 stainless steel was by Michel, Nahm, and Moteff.[25] Specimens showing twin cracks had been tested at 649°C (1200°F) and a strain rate of 8.3×10^{-5}/sec. The average strain rate at which twin cavities were observed in the present investigation varied from 1.6 to 1.9×10^{-7}/sec. Furthermore, specimens showing twins were aged for 10,000 hr at 593 and 649°C (1100 and 1200°F) and both tested at 593°C (1100°F). Although the strain rate used in the present investigation was 0.002 times that used in the investigation of Michel et al.,[25] the twin cavities in both cases were maximum for boundaries inclined between 30 and

---

[23]F. Garofalo, *Ductility*, American Society for Metals, Metals Park, Ohio, 1968, pp. 87–129.

[24]J. N. Greenwood, D. R. Miller, and J. W. Suitter, "Intergranular Cavitation in Stressed Metals," *Acta. Met.* 2: 250–58 (1954).

[25]D. J. Michel, H. Nahm, and J. Moteff, "Deformation Induced Twin Boundary Crack Formation in Type 304 Stainless Steel," *Mater. Sci. Eng.* 11: 97–102 (1973).

90° to the direction of the applied stress, whereas only a few cavities occurred at angles less than 30°. Such an observation is quite consistent with the results[22] concerning the distribution of grain boundary cavities.

A suitable mechanism for twin boundary cavitation should be able to explain the following characteristics of twin boundary cavities:

1. occurrence of cavities primarily along the coherent part of the twin and seldom on the incoherent twin step (see Figs. 10–15),
2. excessive cracking on twins along the maximum shear stress axis,
3. bending of twins containing no incoherent step,
4. the junction of grain and twin boundaries acting as a nucleating site for the twin crack on a bent twin (Figs. 11 and 15),
5. multiple twin boundary cracking [Fig. 13(a)], and
6. the stopping of twin boundary cracks by the grain boundaries or extending to the twin in the next grain, without causing any grain boundary cracking.

Chalmers[26] described the following characteristic features of annealing-twin boundaries. These boundaries have coherent and noncoherent (incoherent) parts. A coherent twin boundary is one that coincides with the plane of symmetry of the twins, that is, the composition plane. This plane is one in which each atom is correctly placed with respect to the lattice of both crystals. The noncoherent twin boundary, on the other hand, is any other boundary between crystals with the twin relationship. The atoms on such boundaries are not as favorably placed with respect to their neighbors, and the energy of the noncoherent boundary would be higher. Chalmers cited the work of Chalmers et al., who observed that noncoherent twin boundaries appear to be similar to the ordinary boundary rather than to the coherent twin boundary in their behavior under thermal etching conditions. It was further mentioned that the energy of the coherent boundary has its characteristic low value only when it is strictly coherent. If its angle is changed even by a small amount, the energy increases very rapidly. Chalmers cited the work of Fullman and Dunn et al. on energy measurement of twin boundaries and showed that the energy of a noncoherent twin boundary was about 0.8 times the grain boundary energy, while the corresponding ratio for a coherent twin boundary was in the range 0.017 to 0.045. Chalmers stated that a much higher value of noncoherent twin boundary energy was not surprising because the distances between nearest neighbors are considerably disturbed when the boundary is not coherent.

From the above discussion it follows that a noncoherent twin boundary can behave just like a grain boundary, and futhermore that the energy of a coherent boundary can be increased sharply by increasing its angle even by a small amount. Since noncoherent twin boundaries are similar to grain boundaries (in their atomic arrangement and energy) sliding along such a boundary can be considered as a possible mechanism for twin boundary cracking, as explained in Fig. 23. Maximum sliding is expected to occur on noncoherent steps along the maximum shear stress axis (45° to the normal stress), and since coherent twin steps are normal to noncoherent

---

[26] B. Chalmers, "Structure of Crystal Boundaries," pp. 293–319 in *Progress in Metal Physics*, Vol. 3: Pergamon, London, 1952.

steps, maximum cracking would be expected to occur on coherent twins along the maximum shear stress axis. Such an interpretation is consistent with the micrographs presented in Figs. 9, 10, 12 and 15. Some of the cracking observed along the twins containing no noncoherent twin step may be due to either sliding along a very small nonobservable step or gross deformation in the grains, which can cause tearing of the coherent boundary. The tearing is possible because precipitation at these boundaries could have changed their angle and thus increased their energy sharply.[26] There is some evidence in Fig. 13(b) of unzipping of the coherent boundary along the precipitate-matrix interface, indicating a low cohesion of small precipitate particles at the twin boundary in the aged condition and at the grain boundaries in the unaged specimen. From the above discussion it follows that large gloublar precipitate particles at grain boundaries of the aged specimen, which did not crack, must have high cohesion.

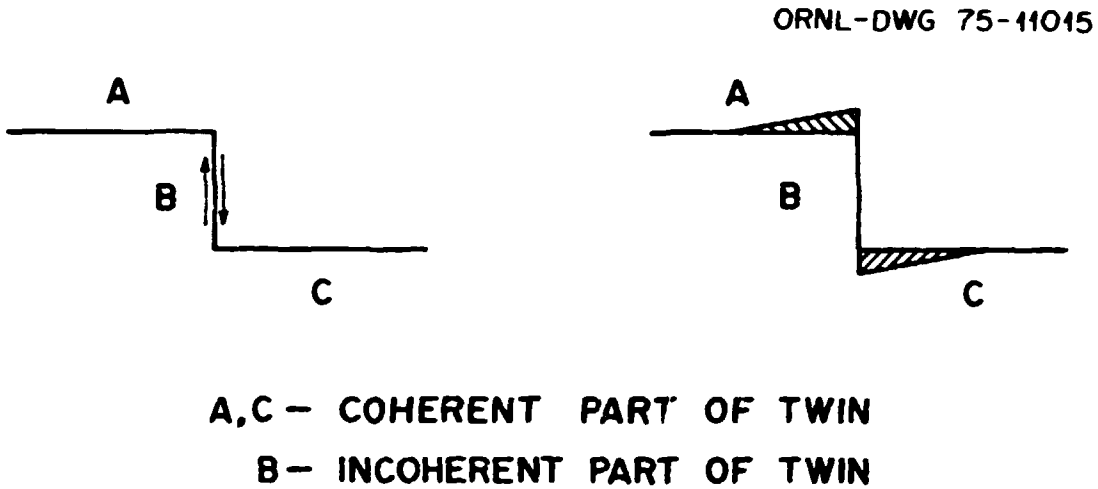

Fig. 23. Noncoherent Twin Boundary Sliding Mechanism for Twin Boundary Cracking.

The results presented thus far have shown that twin boundary cavitation occurs as a result of extensive intragranular deformation. In specimens pretreated for short time at high temperature [i.e., 816°C (1500°F)] the situation is exactly opposite to that observed for the long-term low-temperature-treated case. For example, loading strain was low and intragranular strain high for the long-term low-temperature-treated specimen, whereas loading strain was high and intragranular deformation small for the short-term high-temperature-treated specimen. The specimen treatment for 24 hr at 816°C (1500°F) produced precipitate only at the grain boundaries, whereas aging for long times at 593 and 649°C (1100 and 1200°F) produced precipitates in the matrix and at the grain boundaries.

The difference in precipitation between the long-term low-temperature and short-term high-temperature treatments, Figs. 21 and 22, is considered as the possible cause for transition from twin back to grain boundary cavitation, as was found in the latter (Fig. 16). One important point to note is that precipitate particle size and distribution at the grain boundaries and matrix are critical in determining the nature of creep cavitation of austenitic stainless steels. The most critical combination of precipitates at the grain boundaries and matrix happens for an aging temperature of 649°C (1200°F), where creep-rupture time was minimum, ductility was maximum, and cavitation occurred at the twin boundaries.

Comparison between the tensile and creep ductility of type 304 stainless steel (heat 926) showed that while ductility increased as a result of aging for the creep test, it decreased for a tensile test. Such an observation suggests that ductility increases with decreasing strain rate, which is contrary to the commonly observed decrease in the unaged condition for the identical strain rates. The details of the change in strain rate dependence of the aged condition are discussed elsewhere.[27]

SUMMARY AND CONCLUSIONS

The influence of long-term low-temperature (LtLT) and short-term high-temperature (StHT) treatments on tensile, creep, and fracture properties of type 304 stainless steel were investigated. The (LtLT) was 4000 or 10,000 hr at 482, 593, and 649°C (900, 1100, and 1200°F), whereas StHT treatment was 24 hr at 816°C (1500°F). The following are some general remarks and conclusions.

1. The LtLT treatment slightly increased yield strength at room temperature and 593°C (1100°F), but tensile ductility (uniform and total elongation and reduction of area) was significantly reduced. The StHT treatment decreased the yield strength.

2. Both treatments increased minimum creep rate, lowered time to rupture, and increased creep ductility. The minimum in time to rupture and maximum in minimum creep rate and ductility were observed for a treatment temperature of 649°C (1200°F).

3. Ansell and Weertman's dislocation creep theory for the effect of dispersed particles on minimum creep rate was tried for the aged type 304 stainless steel. The difference between theory and experiment was significant and was suggested to have possibly resulted from the influence of the grain boundary precipitate, which was not considered in the theory.

4. The LtLT treatment at 593 and 649°C (1100 and 1200°F) followed by a creep test at 593°C (1100°F) and 207 MPa (30 ksi) resulted in twin boundary creep cavities in both heats of type 304 stainless steel. Twin boundary creep cavities were also observed in another heat of type 304

---

[27]V. K. Sikka, C. R. Brinkman, and H. E. McCoy, "Effect of Thermal Aging on Tensile and Creep Properties of Types 304 and 316 Stainless Steels," paper to be presented at Symposium on Structural Materials for Elevated Temperature Nuclear Power Generation Service, 1975 ASME Winter Meeting, Houston, Texas, Nov. 30 to Dec. 4, 1975.

stainless steel without any prior treatment. Examples of twin boundary creep cavities in LtLT treated type 316 stainless steel have also been presented.

5. Transmission electron microscopy on the aged specimens was performed to estimate the precipitate size at various sites.

6. The absence of grain boundary cavitation in LtLT treated specimens was suggested to possibly result from

(a) intragranular flow strength being lower than that of the grain boundaries,

(b) possible grain boundary migration between the coarse particles at the grain boundaries, and

(c) more cohesion between the coarse precipitate and the matrix compared with fine precipitates.

7. A sliding mechanism along noncoherent twin boundaries was suggested for twin boundary cavitation. Micrographs consistent with the observed mechanism are presented.

ACKNOWLEDGMENTS

The authors gratefully acknowledge E. B. Patton and E. Lee for performing the creep test, L. T. Ratcliff for performing tensile tests, C. L. Angel, C. W. Houck, and E. Lee for doing metallography, C. L. White, R. L. Klueh, and W. R. Martin for reviewing, Sigfred Peterson for editing, and Regina G. Collins for typing the manuscript.